Potato Research
https://doi.org/10.1007/s11540-024-09748-7

A Systematic Review of Vegetation Indices for Potato Growth Monitoring and Tuber Yield Prediction from Remote Sensing

A. Mukiibi[1] · **A. T. B. Machakaire**[2] · **A. C. Franke**[3] · **J. M. Steyn**[1]

Received: 11 December 2023 / Accepted: 1 June 2024

Abstract

Crop intelligence and yield prediction of potato (*Solanum tuberosum* L.) are important to farmers and the processing industry. Remote sensing can provide timely information on growth status and accurate yield predictions during the growing season. However, there is limited documentation on the most suitable vegetation indices (VIs) and optimal growth stages for acquiring remote sensing imagery of potato. To address this knowledge gap, a systematic review was conducted. Original scientific manuscripts published between 2000 and 2022 were identified using various databases. The findings indicate that satellite imagery is the most widely used source of remote sensing data for tuber yield prediction, whereas unmanned aerial vehicle systems (UAVs) and handheld sensors are more frequently applied for growth monitoring. The normalized difference vegetation index (NDVI), red-edge chlorophyll index ($CI_{red\text{-}edge}$), green chlorophyll index (CI_{green}), and optimized soil-adjusted vegetation index (OSAVI) are the most frequently used VIs for the growth and yield estimation of potato. The tuber initiation stage was found to be the most appropriate stage for remote sensing data acquisition. This review will assist potato farmers, agronomists and researchers in selecting the most suitable VIs for monitoring specific growth variables and selecting the optimal timing during the growing season to obtain remote sensing images.

Keywords Normalized difference vegetation index · Satellite imagery · Unmanned aerial vehicles · Yield prediction

✉ J. M. Steyn
martin.steyn@up.ac.za

[1] Department of Plant and Soil Sciences, University of Pretoria, Hatfield 0028, South Africa

[2] Department of Agriculture, McCain Foods NZ, Hastings 4120, New Zealand

[3] Department of Soil, Crop and Climate Sciences, University of the Free State, Bloemfontein 9300, South Africa

Published online: 22 June 2024

Introduction

Potato (*Solanum tuberosum* L.) growth monitoring and tuber yield prediction are of utmost importance for effective management of crops and planning of farm activities, such as harvesting, storage, distribution, and marketing logistics (Stone and Meinke 2005; Van der Velde and Nisini 2019). Moreover, monitoring potato crop development during the growing season allows for an adaptive management of fertilizers, irrigation, and pests and diseases (van Evert et al. 2012; Cucho-Padin et al. 2020; Gold et al. 2020).

Crop growth monitoring and yield prediction through ground-based observations and destructive sampling during the growing season tend to be costly, time-consuming, and prone to errors (Basso and Liu 2019; Tiedeman et al. 2022). As such, process-based crop models have been developed to simplify growth and yield prediction processes. Well-calibrated crop models can provide reliable estimates of potato growth and tuber yield before harvest (Raymundo et al. 2014). However, calibration for local conditions is necessary to accommodate the spatial variability in soil and weather conditions, crop variety, and management practices, which require a large amount of data input (Boote et al. 1996). These requirements can result in simulation uncertainties if input data are inaccurate or incomplete (Hoogenboom et al. 2019).

Recently, remote sensing technology has been adopted to monitor crop growth and predict yield during the season, and the spectral reflectance of green plants has been related to crop growth variables such as leaf area index (LAI), canopy cover, biomass, leaf chlorophyll content (LCC), and yield (Haboudane et al. 2002; Al-Gaadi et al. 2016; Tenreiro et al. 2021). Various vegetation indices (VIs), such as the normalized difference vegetation index (NDVI), weighted difference vegetation index (WDVI), enhanced vegetation index (EVI), red-edge inflection point (REIP), and ratio vegetation index (RVI) have been derived from remote sensor observations and used as proxies for plant growth and productivity (Prasad et al. 2006; Herrmann et al. 2011; Xue and Su 2017). Although remote sensing has been widely used in crop monitoring, there is a lack of literature regarding the appropriate phenological growth stage for acquiring remote sensing imagery and suitable VIs for optimal potato growth monitoring and tuber yield prediction.

This paper presents a systematic literature review of published original research on the application of remote sensing in potato growth monitoring and yield prediction. The objective of this study was to address the gaps in the existing literature by answering the following research questions:

- What are the most suitable remote sensing techniques for potato growth monitoring and tuber yield prediction?
- What are the most widely used vegetation indices to monitor potato growth and predict yield?
- What is the most appropriate phenological stage for accurate potato yield prediction?

The remainder of this paper is organized as follows. Sect. "Overview of Remote Sensing Applications for Potato" provides an overview of the remote sensing applications for potato growth monitoring and yield prediction. Sect. "Research Methodology" describes the methodology used in the systematic review. Sect. "Results and Discussion" presents the results and discussion, and Sect. "Conclusions" presents the conclusions.

Overview of Remote Sensing Applications for Potato

Remote sensing information can be retrieved using various sensors, such as cameras, video recorders, multispectral and hyperspectral scanners, mounted on satellites, airplanes, unmanned aerial vehicles (UAVs), and ground-based platforms. The application of remote sensing for potato crop monitoring can be categorized into three main areas: growth monitoring, vegetation condition status monitoring, and tuber yield prediction.

Growth Monitoring

Remote sensing is based on acquiring electromagnetic wave reflectance from vegetation surfaces. The reflected light from vegetation surfaces depends on factors such as plant type, growth stage, water content and intrinsic tissue factors. Reflectance within the ultraviolet (10 – 380 nm), the visible region (450 – 750 nm) and the near infrared wave band (850 – 1100 nm), are prominent in agricultural applications (Xue and Su 2017). The change in reflectance at different wavelengths during the different crop growth stages is used to derive VIs that are related to canopy state variables, such as aboveground biomass (AGB), LAI, ground canopy cover, plant height, and vigour assessment (Delegido et al. 2008). The NDVI is the most popular VI related directly or indirectly to growth variables through regression or machine learning (ML) models (Peng et al. 2021a; Tenreiro et al. 2021).

Vegetation Condition Status

Remote sensing has been employed to estimate the leaf nitrogen (N) and LCC of potato crops (Clevers and Kooistra 2012; Kooistra and Clevers 2016). Plant health and vigour are used to assess the plant vegetation condition status. Healthy and vigorous plants usually exhibit rapid emergence, early ground coverage, and high concentrations of leaf N and LCC (Ter Steege et al. 2005; Basu and Groot 2023). Furthermore, leaf N and LCC can serve as indicators of plant nutritional status, photosynthetic rate, and biomass production (Clevers and Kooistra 2012; Kooistra and Clevers 2016). Therefore, in-season measurement of leaf N and LCC using remote sensing can be of great assistance in timely N management and optimising N use efficiency by the crop (van Evert et al. 2012).

Remote sensing has been used to monitor and assess the incidence and severity of diseases in potatoes (Couture et al. 2018; Duarte-Carvajalino et al. 2018; Gold et al.

2020). According to Polder et al. (2019), there is a significant difference between the reflectance of healthy and diseased potato leaves. Plant pathogens (fungi, bacteria, and viruses) attack the epidermal and mesophyll cells of leaves, which affects the biophysical and biochemical properties of crop vegetation (Couture et al. 2018). Disease infection therefore influences the spectral reflectance of vegetation, which in turn affects spectral metrics, such as spectral distance and VIs (Griffel et al. 2018). Simultaneously, spectral reflectance is affected by factors such as water and nutrient stress, natural plant senescence, variability of canopy structure, and spectral resolution of the sensor, which limits the accuracy of disease assessment using remote sensing (Franceschini et al. 2019). Despite these limitations, several studies reported successful disease assessment using high spectral resolution imagery and spectral reflectance classification techniques, including parametric and non-parametric modelling techniques, as well as classification methods, such as quadratic discriminant analysis, support vector machine (SVM), and classification trees (Duarte-Carvajalino et al. 2018; Franceschini et al. 2019). Griffel et al. (2018) and Couture et al. (2018) used support vector machine classification methods and found that potato plants infected with potato Virus Y (*Potyviridae* PVY) had significantly lower reflectance values between 700 – 1300 nm wavelengths than healthy plants. Other foliar diseases including potato early blight (*Alternaria solani*) (Van De Vijver et al. 2020) and late blight (*Phytophthora infestans*) (Franceschini et al. 2017a, b; Gold et al. 2020; Hou et al. 2022) have been monitored using remotely sensed data.

Remote sensing has been used to assess plant water status and water stress in crops (Gerhards et al. 2016). This can be achieved through the estimation of leaf water content using indicators such as water potential, relative water content, equivalent water thickness of leaves and canopy temperature (Ahmad et al. 2021). Moreover, remote sensing can provide information for estimating crop water requirements through the determination of crop evapotranspiration (ET) (Jayanthi et al. 2007; Campos et al. 2017; Pôças et al. 2020). Knowledge of crop ET facilitates irrigation scheduling. Crop ET can be estimated through remote sensing using two approaches. The first approach involves using thermal bands as inputs to the surface energy balance algorithm for land (SEBAL), mapping evapotranspiration at high resolution using internalized calibration (METRIC), surface energy balance index (SEBI), and surface energy balance system (SEBS) (Bastiaanssen et al. 1998; Allen et al. 2005; Aryalekshmi et al. 2021). The required energy fluxes (net radiation Rn, soil heat flux, and sensible heat H) are derived from satellite images (Allen et al. 2011; Irmak et al. 2011). Successful applications of energy balance models for estimating ET in various crops have been reported (Bastiaanssen et al. 2005; Tasumi et al. 2005; Tasumi and Allen 2007; Bashir et al. 2008; Kumar et al. 2020). Although this approach provides a precise measure of crop ET, it requires extensive data input and is limited by the availability of satellites equipped with thermal sensors (Glenn et al. 2010).

The second method entails estimating crop coefficients (the single crop coefficient, Kc, and the basal crop coefficient, Kcb) based on VIs (VI approach) (Jayanthi et al. 2007; Mukiibi et al. 2023). The VI-based Kc or Kcb values are then multiplied by the reference evapotranspiration to determine ET. Relationships between VIs and crop coefficients have been established for various crops using linear and nonlinear

equations (Choudhury et al. 1994; Duchemin et al. 2006; Campos et al. 2017). The VI approach is relatively simple and requires fewer computations than the surface energy balance models (Glenn et al. 2010). However, reductions in ET due to stomatal closure, particularly during periods of water deficit, cannot be detected using the VI approach (González-Dugo and Mateos 2008).

Yield Prediction

Remote sensing techniques have been employed to forecast and predict crop yields using linear and non-linear models. The most common models for remote sensing applications are empirical relationships between VIs and final yield (Lobell 2013). However, empirical models require calibration using ground measured data for accurate yield predictions. A major limitation of empirical models is that they are site-specific and may not provide accurate yield predictions in different locations and years (Basso et al. 2013). Recent advancements in data processing techniques using ML algorithms have led to the development of more precise yield prediction models that incorporate VIs and factors that affect crop yields, such as fertilizer application rates (nitrogen, phosphorus, and potassium), irrigation, soil properties, weather parameters, and crop management information (plant population) (Abrougui et al. 2019; Abbas et al. 2020; Muruganantham et al. 2022). Additionally, these factors have a significant influence on the spectral reflectance of the crop canopy and can be used to explain the spatial variability in crop yields.

Remotely sensed information can also be incorporated into a crop simulation model during calibration, or to adjust the initial conditions of the model (Doraiswamy et al. 2003; Pinter et al. 2003; Awad 2019). The integration of remotely sensed data into process-based crop models can provide more accurate results than using process-based crop models alone (Launay and Guerif 2005; Dente et al. 2008; Jin et al. 2018). For instance, canopy state variables and soil moisture can be integrated into potato models to enhance the yield prediction accuracy (Dente et al. 2008; Jin et al. 2016; 2018; Zhou et al. 2017b).

Research Methodology

This study followed the systematic review guidelines outlined by Kitchenham and Charters (2007). Additionally, the study followed the preferred reporting items for systematic reviews and meta-analyses (PRISMA) (Liberati et al. 2009). The PRISMA framework describes the flow of information through the different phases of a systematic review, and includes article identification, screening, eligibility, and data analysis (Fig. 1).

Article Search Procedure

A literature search was performed on the internet using the following databases: Google Scholar, ScienceDirect, Scopus, Web of Science, IEEE Explorer, MDPI,

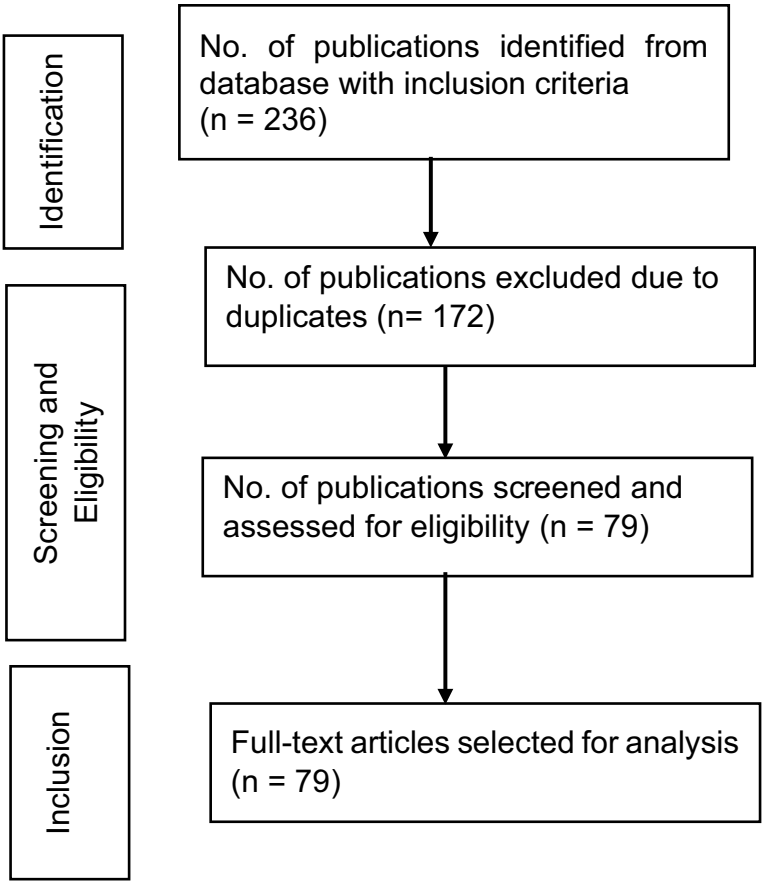

Fig. 1 The PRISMA flow diagram indicating the number of articles in each phase of the selection process

Taylor and Francis, and SpringerLink. More studies were sourced by scanning the reference lists of articles obtained from the databases. Databases were selected based on the comprehensiveness of archiving and accessibility. This research focused on potato yield prediction using remote sensing technologies; therefore, the search strategy in the databases included keywords and Boolean operators "AND" and "OR" with the main search string as "potato yield prediction" AND "remote sensing". As a consequence, less emphasis was put on vegetation condition status. To include any other relevant articles in our study, the search string was modified by adding the following keywords: "potato yield prediction" OR "potato yield forecasting" OR "potato yield estimation" AND "remote sensing" OR "satellite imagery." Minor adjustments were made to the search string to suit each database (Table 1). Original research studies conducted between 2000 and 2022 were used for this study, as the use of remote sensing technologies in agriculture gained momentum with the launch of MODIS and Landsat-7 satellite sensors in 1999 (Kasampalis et al. 2018;

Table 1 Search string and number of papers retrieved from each database

Database	Search string	Total Papers	No. after exclusion criteria	No. after removing duplicates
MDPI	(’potato yield prediction’ OR ’potato yield estimation’ OR ’potato yield forecast*’ AND ’remote sensing’)	1631	27	24
ScienceDirect	(’potato yield prediction’) OR (’potato yield estimation’) OR (’potato yield forecasting’)) AND ((’Remote sensing’) OR (’satellite imagery’)	1140	29	19
Web of Science	TS = (’potato yield prediction’ OR ’potato yield estimation’ OR ’potato yield forecast*’ AND ’remote sensing’)	517	78	2
Wiley Online library	"’potato yield prediction’ OR ’potato yield estimation’ OR ’potato yield forecast*’) AND (’remote sensing’)" anywhere	370	4	3
Taylor and Francis	[All: ’potato yield prediction’] AND [All: and remote] AND [[All: sensing] OR [All: ’satellite]] AND [All: imagery"] AND [Article Type: Article]	357	8	7
SpringerLink	(’potato yield prediction’ OR ’potato yield estimation’ OR ’potato yield forecast*’) AND (’remote sensing’)’	319	16	13
Google Scholar	potato yield prediction’’ OR potato yield estimation" OR "potato yield forecasting" AND "Remote sensing" OR "satellite imagery"	100	60	6
Scopus	(TITLE-ABS-KEY (’potato AND yield AND prediction’) OR (’potato AND yield AND estimat*’) OR (’potato AND yield AND forecast*’) AND (’remote AND sensing’) OR (’satellite AND imagery’))	28	9	0
IEEE *X*plore	(’potato yield prediction’ OR ’potato yield estimation’ OR ’potato yield forecast*’ AND ’remote sensing’)	20	5	5
Total		**4482**	**236**	**79**

Khanal et al. 2020). Since then, various remote sensing platforms, including satellites, manned and UAVs, have been developed and used to collect vegetation spectral data for different precision agricultural applications.

Article Selection Criteria

The search query in each database returned several inapplicable records, most of which were out of the scope (Table 1). To be included, studies had to meet the minimum criteria of including remote sensing applications for potato growth and yield prediction. Publication titles, abstracts, and keywords were used to select articles for further analysis. Articles were excluded using the following criteria:

- Articles not focused on potato.
- Studies not including remote sensing data or remote sensing applications not related to growth monitoring or yield prediction.
- Publications without access to the full-text version, review articles, and articles in a language other than English.

Data Analysis

The number of articles published per annum and the number of articles per remote sensing application were calculated. Information that answered the research questions was extracted from the publications. A bibliometric analysis was conducted using VOSviewer software (www.vosviewer.com, van Eck and Waltman 2010) to identify authors' keywords appearing in three or more publications. This allowed the visualization of the network between the most dominant themes in remote sensing applications for potato research.

Results and Discussion

Descriptive Statistics of Selected Publications

The number of publications on remote sensing application in potato increased rapidly in recent years (Fig. 2). After applying the inclusion criteria, 79 articles were selected for further analysis. Remote sensing was mainly used for potato yield prediction (37% of the total studies), followed by leaf N status estimation (21% of the total studies) (Fig. 3). The most frequently used keywords related to growth and yield prediction were potato yield, tuber yield, LAI, plant height, AGB, and phenology (Fig. 4). Other common keywords included remote sensing, machine learning, precision agriculture, random forest, climate change, and UAV.

The use of remote sensing technology to monitor crop growth and predict yield is rooted in the premise that remotely sensed features, mainly spectral reflectance, VIs and canopy texture, can serve as proxies for plant growth variables, such as LAI, AGB, and fraction of photosynthetically active radiation (fPAR) (Lobell 2013; Zhou

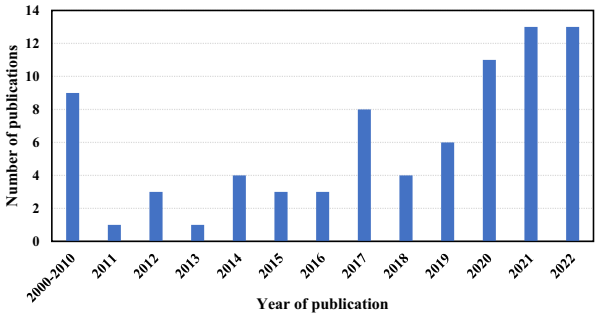

Fig. 2 Number of publications from 2000 to 2022 included in the review

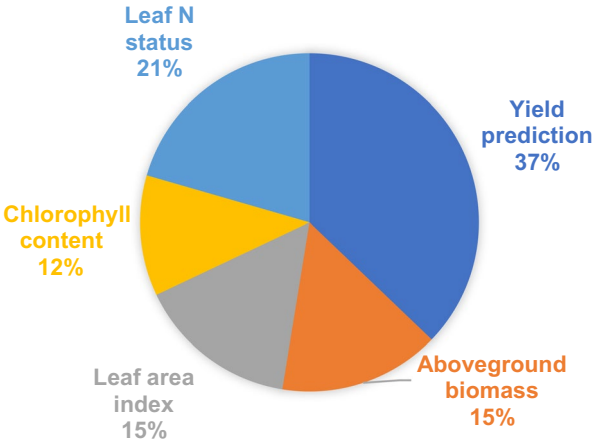

Fig. 3 Distribution of growth monitoring and yield prediction aspects from selected articles

et al. 2018). These plant growth variables play a vital role in biophysical processes, such as light interception, photosynthetic activity, and biomass accumulation, which directly affect final crop yield (Mulla 2013; Vannoppen and Gobin 2022). Remote sensing enables the real-time observation of vegetation condition, which is influenced by both crop genetics and management practices (Zhou et al. 2018). As VIs are linked to the primary productivity of crops, potato yield prediction using various models based on VIs has been explored (Table 2).

Potato Yield Prediction

Remote Sensing Techniques for Potato Yield Prediction

Optical satellite systems were the most widely used remote sensing platforms for predicting yield (Table 2). Sentinel-2 was the most popular satellite platform, while other platforms adopted by researchers included Landsat satellite series 5–8, Planet Scope, National Oceanic and Atmospheric Administration (NOAA) equipped with

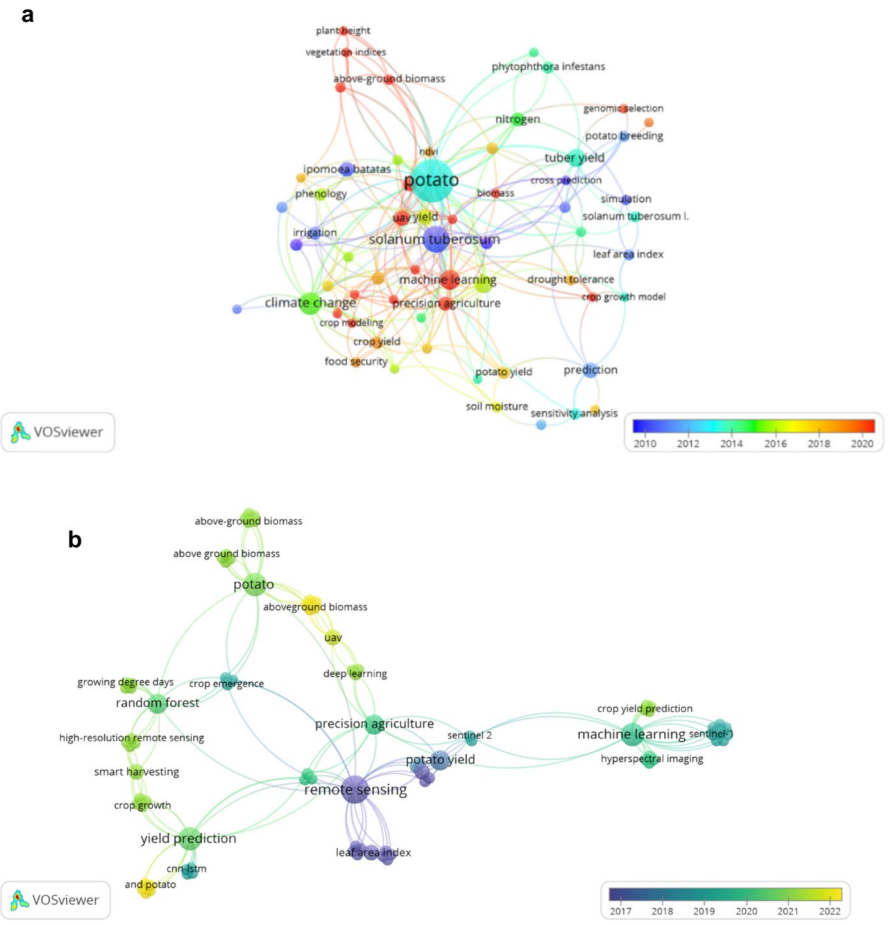

Fig. 4 Overlay visualization of co-occurrence of author keywords from the Web of Science (**a**) and Scopus (**b**) databases

an Advanced Very High-Resolution Radiometer (AVHRR) sensor, TERRA, and Aqua satellites equipped with moderate-resolution imaging spectroradiometer (MODIS) sensors (Table 2). Optical satellite platforms are equipped with high-resolution multispectral sensors that capture fine-scale details of crop vegetation over large areas, facilitating potato yield prediction at both the field and regional scales (Salvador et al. 2020). However, the main limitation of optical satellite platforms is the trade-off between acquiring images with sufficiently high spatial and temporal resolution to obtain multiple cloud-free images during the growing season (Lobell et al. 2007; Mulla 2013; Khabbazan et al. 2019). For example, Sentinel-2 satellites have a temporal resolution of 5 days and a relatively high spatial resolution (10 or 20 m/pixel for land applications) (Herrmann et al. 2011; Sun et al. 2022). Landsat satellites have a relatively high spatial resolution of 30 m/pixel, but a low temporal resolution of 16 days. The TERRA satellite has a high temporal resolution of 1

Table 2 Summary of the remote sensing types and models used for potato yield prediction and model accuracy

Data source	Models & Features	Prediction accuracy[a]	Reference
Landsat-8 and Sentinel-2 satellites with multi-spectral sensors	Linear regression analysis using NDVI, VCI and SAVI	$R^2 = 0.65–88$	Al-Gaadi et al. 2016; Kumar et al. 2019
Landsat-5–8 Time series images	Regression analysis with NDVI	$R^2 = 0.81$	Newton et al. 2018
PlanetScope and Sentinel 2 satellite with multi-spectral sensors	OLSR_NDVI, GNDVI, SAVI, MSAVI2	$R^2 = 0.57$	(Abou Ali et al. 2020)
TERRA satellite with MODIS multispectral sensors	Linear regression with NDVI, LAI and fPAR. ML_ NDVI and weather data	$*R^2 = 0.84–0.86$	(Bala and Islam 2009; Salvador et al. 2020)
Terra and Aqua satellite with MODIS	Linear regression_NDVI and EVI	$R^2 = 0.70–0.82$	(Johnson 2016)
Sentinel-2 Multispectral sensor	ML: SVMR, RF_ multiple VIs and PPI. RF with NDVI and weather data. PCA_Multiple VIs	$*R^2 = 0.56–0.93$	(Gomez et al. 2019; Mhango et al. 2021; Vannoppen and Gobin 2022)
Sentinel-1&2	GEE and backscattering technique using AUROC, ML: SVMR, LR, RF_NDVI	$R^2 = 0.95$	(Singha and Swain 2022; Singha et al. 2022)
AVHRR	Linear regression and PCR using TCI and VCI	$R^2 = 0.75$	(Rahman et al. 2012)
Ground based FieldScout NDVI meter	ML: LR, SVR, K-NN and EN with NDVI and soil properties	$*R^2 = 0.54–0.72$	(Abbas et al. 2020)
Ground-based hyperspectral Spectrometer	Integrated genetic algorithm GA- ANFIS models with 20 VIs	$R^2 = 0.70–0.97$	(Elsayed et al. 2021b)
Ground-based infrared thermal and RGB digital cameras	GA-ANFIS model with RGB VIs and stepwise MLR	$R^2 = 0.72–1.00$	(Elsayed et al. 2021a)
Ground-based FieldSpec Pro spectrometer	MLR_biomass and VI	$*R^2 = 0.67$	(Li et al. 2020a)
Ground-based USB 2000 Spectrometer	Six VIs, LAI and growth stage weighting methods	$*R^2 = 0.70–0.85$,	(Luo et al. 2020)
Ground-based GreenSeeker and Holland Scientific Crop Circle™ ACS-430 sensors	Regression analysis with NDVI, NDVI*LAI, NDRE, & CI	$R^2 = 0.70–081$	(Sharma et al. 2017; Zaeen et al. 2020; Satognon et al. 2021)
UAV with hyperspectral sensor	ML: RR_Multiple VIs	$R^2 = 0.63$	(Sun et al. 2020)
UAV with multispectral sensor	Regression_ NDVI and plant height	$R^2 = 0.99$	(Tanabe et al. 2019)

Table 2 (continued)

Data source	Models & Features	Prediction accuracy[a]	Reference
UAV with multispectral sensor	Regression analysis and ML: RF; SVR, with multiple VIs and cultivar type	*R^2 = 0.79–0.95	(Li et al. 2021b, a)

MODIS is Moderate Resolution Imaging Spectroradiometer, *AVHRR* is Advanced Very High-Resolution Radiometer, *OLSR* is ordinary least squares regression, *LAI* is leaf area index, *fPAR* is fraction of intercepted photosynthetic active radiation, *ML* is machine learning, *PPI* is potato productivity index, *RF* is random forest, *PCA* is principal component analysis, *GEE* is google earth engine, *SVMR* is support vector machine radial, *LR* is linear regression, *PCR* is principal component regression, *TCI* is temperature condition index, *VCI* is vegetation condition index, *SVR* is support vector regression, *K-NN* is K-nearest neighbour, *EN* is elastic net, *GA-ANFIS* is genetic algorithm -adaptive neuro-fuzzy inference system, *RGB* is red–green–blue, *MLR* is multiple linear regression, *VIs* is vegetation indices, *CI* is chlorophyll index, *AUROC* is area under receiver operating characteristic curve, *OCW* is optimal combination weighting method, *RR* is ridge regression and *SGI* is sum green index. [a]Note: the R^2 values with an asterisk (*R^2) indicate the total variance explained by multiple variables, including VIs and non-remote sensing features in a predictive model

– 2 days but a low spatial resolution of 250 – 1000 m/pixel. The Planet Scope satellite provides images with the highest spatial resolution (3 m/pixel) and highest temporal resolution (daily). However, these images are costly ($218 per 100 km^2), limiting the use of Planet Scope images for agricultural monitoring (Sun et al. 2022).

Owing to the limitations of optical remote sensing, microwave (radar) sensors, which can penetrate clouds with high spatial and temporal resolution and are independent of light conditions, have been investigated for Earth observations (Bouman and van Kasteren 1990; Clevers and Van Leeuwen 1996; Steele-Dunne et al. 2017). Microwave remote sensing uses synthetic aperture radar (SAR) sensors that emit low-frequency microwave pulses (1 – 10 GHz) towards the Earth's surface (Steele-Dunne et al. 2017; Khabbazan et al. 2019). The pulses are scattered upon interaction with different surfaces (vegetation and soil) and sent back to the receiver, which is also known as radar backscattering (Moran et al. 2002). Radar backscattering from a vegetation surface is mainly influenced by canopy size, ridge orientation, architecture of individual plants, crop type, growth stage, water content of the plant parts, and roughness of the vegetation canopy (Bouman and van Kasteren 1990). Radar backscattering by the soil surface is mainly influenced by soil water content and surface roughness. Therefore, radar remote sensing has potential for agricultural applications, particularly for crop monitoring, classification, and soil/vegetation moisture estimation (Moran et al. 2002; Steele-Dunne et al. 2017). With the launch of the Sentinel-1 satellites (Sentinel-1A and Sentinel-1B), high temporal (6 – 12 days), and high spatial (2.3 – 13.9 m) SAR data can be freely accessed in different parts of the world (Mercier et al. 2020). The potential of Sentinel-1 SAR data for monitoring phenological development of various crops including maize, potato, sugar beet, winter wheat, rapeseed and rye grass was evaluated by Khabbazan et al. (2019) and Mercier et al. (2020). Radar backscattering coefficients can be used to estimate crop growth variables such as crop height (Abdikan et al. 2018; Arslan et al. 2022), crop biomass (Ndikumana et al. 2018), LAI (Clevers and Van Leeuwen 1996; Hirooka et al. 2015), and crop yield (Clevers and Van Leeuwen 1996).

Besides optical satellites, ground-based systems were the second most widely used platforms, including the Field Scout NDVI meter, handheld hyperspectrometers, infrared cameras, red, green, and blue (RGB) digital cameras, GreenSeeker, and Holland Scientific Crop Circle™ sensors (Table 2). Ground-based remote sensing devices provide benefits such as high spatial resolution, real-time data, cost-effectiveness for small research plots, control over measurement conditions, and access to ground-truth measurements, which can be used to validate and improve the accuracy of potato yield prediction (Sun et al. 2022).

The Most Used Vegetation Indices for Potato Yield Prediction

A wide range of VIs was used to predict potato yield (Table 3). NDVI was the most widely used index (Tables 2 and 3). Other commonly used indices included GNDVI, normalized difference red-edge (NDRE), SAVI, EVI, red-edge chlorophyll index ($CI_{red\text{-}edge}$) and RVI (Table 3).

The accuracy of final tuber yield prediction was evaluated based on the coefficient of determination (R^2) between VI and observed yields. The ranges of R^2

Table 3 Most widely used vegetation indices for estimating potato yield, aboveground biomass, leaf area index, and canopy chlorophyll

Index	Code	Formula
Normalized difference vegetation index	NDVI	$\frac{\mathrm{NIR}-\mathrm{R}}{\mathrm{NIR}+\mathrm{R}}$
Optimized soil-adjusted vegetation index	OSAVI	$1.16 * \frac{\mathrm{NIR}-\mathrm{R}}{\mathrm{NIR}+\mathrm{R}+0.16}$
Re-normalized difference vegetation index	RDVI	$\frac{\mathrm{NIR}-\mathrm{R}}{\mathrm{NIR}+\mathrm{R}}^{0.5}$
Modified simple ratio	MSR	$\frac{\left(\frac{NIR}{R}\right)-1}{\left(\frac{NIR}{R}\right)^{0.5}+1}$
Soil adjusted vegetation index	SAVI	$1.5 * \frac{\mathrm{NIR}-\mathrm{R}}{\mathrm{NIR}+\mathrm{R}+0.5}$
Triangular vegetation index	TVI	$0.5[120(NIR-G)-200(R-G)]$
Spectral polygon vegetation index	SPVI	$0.4[3.7(NIR-R)-1.2(R-G)]$
Ratio vegetation index	RVI	$\frac{\mathrm{NIR}}{\mathrm{R}}$
Modified chlorophyll absorption ratio index	MCARI	$\left[\left(\lambda_{700}-\lambda_{670}\right)-0.2\left(\lambda_{700}-\lambda_{550}\right)\right]\left(\frac{\lambda_{700}}{\lambda_{670}}\right)$
Structure-insensitive pigment index	SIPI	$\frac{\mathrm{NIR}-\mathrm{B}}{\mathrm{NIR}+\mathrm{R}}$
Visible atmospherically resistance index	VARI	$\frac{\mathrm{G}-\mathrm{R}}{\mathrm{G}+\mathrm{R}-\mathrm{B}}$
Green NDVI	GNDVI	$\frac{\mathrm{NIR}-\mathrm{G}}{\mathrm{NIR}+\mathrm{G}}$
Enhanced vegetation index	EVI	$2.5 * \frac{\mathrm{NIR}-\mathrm{R}}{\mathrm{NIR}+6\mathrm{R}-7.5\mathrm{B}+1}$
Linear combination index	LCI	$\frac{\left(\lambda_{850}-\lambda_{710}\right)}{\left(\lambda_{850}+\lambda_{670}\right)}^{0.5}$
Normalized difference red-edge	NDRE	$\frac{\mathrm{NIR}-\mathrm{Rededge}}{\mathrm{NIR}+\mathrm{Rededge}}$
Modified soil adjusted vegetation index	MSAVI	$\frac{2NIR+1-\sqrt{(2NIR+1)^2-8(NIR-R)}}{2}$
Normalized difference index	NDI	$\frac{\left(\lambda_{850}-\lambda_{710}\right)}{\left(\lambda_{850}+\lambda_{670}\right)}$
Normalized green–red difference index	NGRDI	$\frac{\mathrm{G}-\mathrm{R}}{\mathrm{G}+\mathrm{R}}$
Red-edge chlorophyll index	$\mathrm{CI}_{\text{red-edge}}$	$\left(\frac{\lambda_{780}}{\lambda_{710}}\right)-1$
Weighted difference vegetation index	WDVI	$\lambda_{870}-\left[\left(\frac{\lambda_{870soil}}{\lambda_{670soil}}\right) * \lambda_{670}\right]$
Wide dynamic range vegetation index*	WDRVI	$\frac{a*\mathrm{NIR}-\mathrm{R}}{a*\mathrm{NIR}+\mathrm{R}}$
MERIS terrestrial chlorophyll index	MTCI	$(\lambda_{754}-\lambda_{700})/(\lambda_{700}-\lambda_{680})$
Photochemical reflectance index	PRI	$\frac{\left(\lambda_{570}-\lambda_{531}\right)}{\left(\lambda_{570}+\lambda_{531}\right)}$
Red-Edge Inflection Point	REIP	$700+40\left\{\frac{\left[\frac{\left(\lambda_{670}+\lambda_{780}\right)}{2}\right]-\lambda_{700}}{\lambda_{740}-\lambda_{700}}\right\}$
Ratio TCARI/OSAVI	TCARI/OSAVI	$\frac{3\left[\left(\lambda_{700}-\lambda_{670}\right)-0.2\left(\lambda_{700}-\lambda_{550}\right)\left(\frac{\lambda_{700}}{\lambda_{670}}\right)\right]}{1.16*\frac{\mathrm{NIR}-\mathrm{R}}{\mathrm{NIR}+\mathrm{R}+0.16}}$
Chlorophyll vegetation index	CVI	$(\lambda_{870} * \lambda_{670})/(\lambda_{550} * \lambda_{550})$
Ratio MCARI/OSAVI	MCARI/OSAVI	$\frac{\left[\left(\lambda_{700}-\lambda_{670}\right)-0.2\left(\lambda_{700}-\lambda_{550}\right)\right]\left(\frac{\lambda_{700}}{\lambda_{670}}\right)}{1.16*\frac{\mathrm{NIR}-\mathrm{R}}{\mathrm{NIR}+\mathrm{R}+0.16}}$
Transformed chlorophyll absorption in reflectance index	TCARI	$3\left[\left(\lambda_{700}-\lambda_{670}\right)-0.2\left(\lambda_{700}-\lambda_{550}\right)\left(\frac{\lambda_{700}}{\lambda_{670}}\right)\right]$
Plant senescence reflectance index	PSRI	$(\lambda_{680}-\lambda_{500})/\lambda_{750}$

Table 3 (continued)

Index	Code	Formula
Canopy chlorophyll content index	CCCI	$\frac{(NDRE)-(NDRE_{Min})}{(NDRE_{Max})-(NDRE_{Min})}$
Ratio at red-edge	R740/720	$\lambda_{740}/\lambda_{720})$
Modified chlorophyll absorption in reflectance index 2	MCARI2	$\frac{1.5[2.5(\lambda_{800}-\lambda_{670})-1.3(\lambda_{800}-\lambda_{550})]}{\sqrt{\left[(2\lambda_{800}+1)^2-(6\lambda_{800}-5(\lambda_{670})^{0.5})-0.5\right]}}$
Green-chlorophyll index	CI_{green}	$\left(\frac{\lambda_{780}}{\lambda_{550}}\right)$

NIR is reflectance in near-infrared band, *R* is reflectance in red band, G is reflectance in green band, B is reflectance in blue band λ_x is reflectance at specified waveband and′*a*′is a weighting coefficient with a value ranging from 0.1 – 0.2

values reported for the six most commonly used VIs are shown in Fig. 5. Positive associations between NDVI and final potato yield had R^2 values ranging from 0.23 – 0.84 (median of 0.67). Relating NDVI (median $R^2 = 0.67$) with final potato yield provided a higher median R^2 than other comparable indices, such as GNDVI (median $R^2 = 0.58$ and NDRE (median $R^2 = 0.61$), despite the fact that NDVI is influenced by soil background reflectance and tends to saturate at LAI values greater than 3 (Gitelson 2004).

A few studies used NDRE to predict yield and reported R^2 values between 0.12 – 0.85 (median of 0.61) (Fig. 5). For instance, Luo et al. (2020) observed a strong association between NDRE and tuber yield ($R^2 = 0.85$) during the starch accumulation stage (80 – 100 DAP). The R^2 for the association between GNDVI and tuber yield ranged between 0.26 – 0.75 (median of 0.58). This indicates that the spectral absorbance of the green portion of the electromagnetic spectrum can be used to predict the final tuber yield. This is supported by Mhango et al. (2021), who reported that the absorbance of the green portion of the magnetic spectrum is significantly associated with the tuber yield. The EVI and $CI_{red\text{-}edge}$ also showed good associations with the tuber yield ($R^2 = 0.4 – 0.87$). Luo et al. (2020)

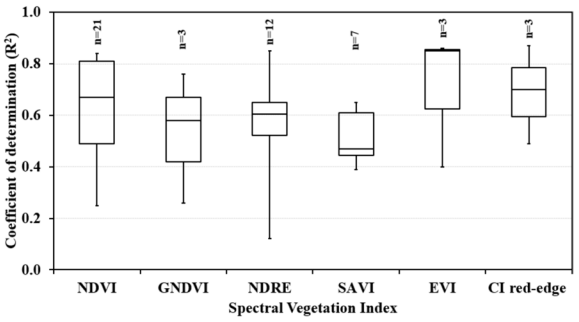

Fig. 5 The coefficient of determination (R^2) for vegetation indices used in final tuber yield prediction (NDVI is normalized difference vegetation index, GNDVI is green NDVI, NDRE is Normalized difference red-edge, SAVI is soil-adjusted vegetation index, EVI is enhanced vegetation index, and $CI_{red\text{-}edge}$ is red-edge chlorophyll index)

estimated potato yield using six VIs and identified $CI_{red\text{-}edge}$ as the best index for potato yield estimation at any growth stage of the crop, with R^2 greater than 0.70.

Preferred Growth Stage for Potato Yield Prediction Using Remote Sensing

The results in Fig. 6 show variability in the R^2 values obtained for the relationship between tuber yield and VIs as the number of days after planting increased from 35 – 95 DAP. The highest median R^2 values were observed between 36 – 55 DAP. These findings suggest that the optimal growth stage for obtaining VIs to predict tuber yield often occurs approximately during maximum ground cover and tuber initiation.

Dry matter accumulation in potato is a function of intercepted photosynthetically active radiation, which exponentially increases to a maximum at 100% ground cover (Haverkort 2018). For most potato varieties, maximum ground cover is attained between 60 – 80 DAP, which also coincides with the peak spectral reflectance and peak VI values reported for potato (Mhango et al. 2022). The reflectance in the NIR region may be inconsistent in the early stages of potato because of the influence of soil background reflectance (Morier et al. 2015). Additionally, the biophysical and biochemical composition of the leaves, which are responsible for light absorption and reflection, are immature during the early stages of the crop, resulting in low absorption of red light and low NIR reflectance (Gómez et al. 2021). Therefore, VIs obtained during the early stages (0 – 40 DAP) of the crop may provide less reliable yield predictions.

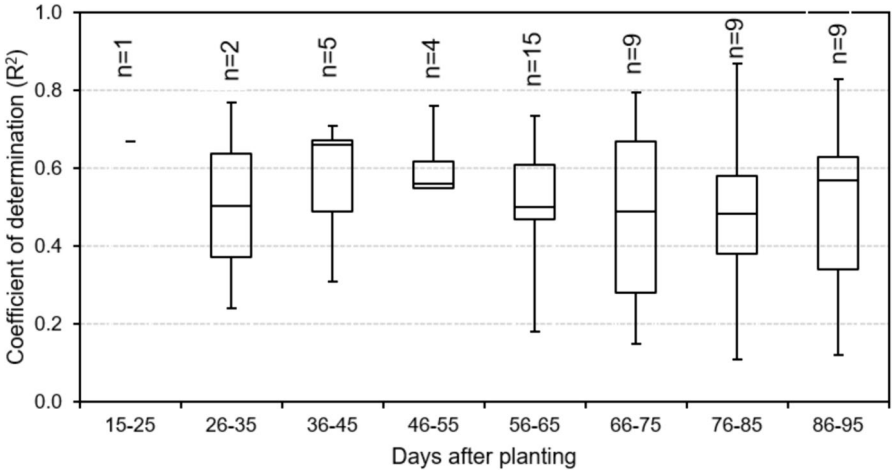

Fig. 6 Box plot comparing the coefficients of determination (R^2) between tuber yield and all vegetation indices combined on different days after planting

Potato Aboveground Biomass Monitoring

Remote Sensing Techniques for Aboveground Biomass Monitoring

Aboveground biomass (AGB) is an agronomic variable widely used to assess crop growth and development, physiological conditions, light use efficiency, and the effects of agricultural management practices, as well as to estimate crop yields (Poorter et al. 2012; Gnyp et al. 2014; Liu et al. 2022a). AGB is also important for determining the nitrogen nutrition index (NNI), which is used to monitor crop N status (van Evert et al. 2012; Jin et al. 2021; Sun et al. 2022). Conventional methods for estimating AGB involve destructive plant sampling, which is time-consuming, labour-intensive, and often unable to detect spatial and temporal variability (Gnyp et al. 2014). Alternative methods for estimating AGB include process-based crop models; however, these models often require numerous inputs that are not readily available for accurate AGB estimation (Craufurd et al. 2013; Wan et al. 2021).

Remote sensing technology provides real-time and non-destructive AGB measurements (Table 4), which are based on the hypothesis that the spectral reflectance of vegetation at specific wavelengths is strongly associated with LAI, canopy coverage, fPAR, and CCC, which are related to crop biomass production (Weiss et al. 2020; Shu et al. 2023). Changes in the spectral reflectance of vegetation at different growth stages are mainly influenced by the biochemical properties of the leaf, such as leaf pigments, water content, and dry matter content, and canopy structure properties, such as LAI and leaf inclination (He et al. 2021; Jin et al. 2021).

Unmanned aerial vehicles (UAVs) were the most commonly used platforms for the in-season estimation of potato AGB (Table 4). UAVs allow frequent and timely monitoring, are easy to operate, and usually provide images with higher spatial and temporal resolution than satellite imagery (Liu et al. 2022b). UAVs can fly at low altitudes to capture images with an extremely high spatial resolution of up to 1 cm/pixel. These images contain vital information regarding the spatial distribution of plants, soil coverage, and canopy structure, which are essential factors for estimating the AGB (Turner et al. 2012; Yu et al. 2016). UAVs are usually equipped with digital, multispectral, and hyperspectral sensors that capture images of varying properties. In particular, hyperspectral sensors have narrow spectral bands that allow visualization of spatial variability in the canopy structure and are highly sensitive to reflected light across the bands (Liu et al. 2022a). Hyperspectral sensors provide shortwave (1100 – 2500 nm) plant spectra, which are strongly associated with leaf water content, lignin, cellulose, and starch content (Gnyp et al. 2014; Marshall and Thenkabail 2015). These leaf traits are directly related to fresh and dry leaf weight. However, the use of hyperspectral sensors is limited because of the large number of spectral bands, high cost, and image processing difficulties (Jin et al. 2021; Mao et al. 2021). Moreover, because UAVs operate at low altitudes, images typically exhibit a small field of view (Turner et al. 2012). Consequently, many images must be captured to adequately cover the required area of interest. The processing of a large number of images necessitates the use of techniques, such as mosaicking, geometric correction, and ortho-rectification, which can be particularly challenging (Turner et al. 2012; Zhang and Kovacs 2012).

Table 4 Comparison of types of remote sensing, models, and main input features for aboveground potato biomass monitoring

Data source	Models and main features	Prediction accuracy[a]	References
UAV_digital RGB cameras	ML _ canopy texture and plant height	*R^2 = 0.71–0.78	(Liu et al. 2022c; b)
UAV_multispectral sensors	Regression and ML (RF)_Texture, geometric features data, VIs and FDV	*R^2 = 0.90	(Luo et al. 2022)
UAV_hyperspectral sensors and RGB Cameras	Regression and ML (RF, GPR, PLSR) _plant height, VIs	*R^2 = 0.60–0.90	(Li et al. 2020b; Liu et al. 2022a; b)
UAV-LiDAR	3DPI Algorithm	R^2 = 0.24	(ten Harkel et al. 2020)
Ground-based FieldSpec hyperspectrometers	Regression and ML _Multiple VIs	R^2 = 0.63–0.88	(Pei et al. 2019; Li et al. 2020a; Yang et al. 2021)
Ground-based Rapid scan, UAV and Sentinel-2 satellite_multi- and hyper-spectral and sensors	Carnegie-Ames-Stanford approach and RVI	R^2 = 0.65–0.85	(Peng et al. 2021b)

UAV is unmanned aerial vehicle, *RGB* is red-green and blue, *VIs* is vegetation indices, *ML* is machine learning, *RF* is random forest, *3DPI* is 3-dimensional profile index, *RVI* is ratio vegetation index, *PSLR* is partial least square regression, *GPR* is Gaussian process regression and *FDV* is Frequency-domain variable. [a]Note: the R^2 values with an asterisk (*R^2) indicate the total variance explained by multiple variables, including VIs and non-remote sensing features in a predictive model

Some studies employed ground-based sensors, specifically handheld field spectroradiometers, for potato AGB estimation (Table 4). Ground-based sensors provide high temporal and spectral resolution images for extracting canopy traits, such as plant height and texture features, which are related to AGB (Liu et al. 2022b, c). However, ground-based sensors are unable to capture large-scale images that illustrate the spatial distribution of crop growth (Zhu et al. 2019). Furthermore, image acquisition using ground-based sensors often results in damage to crops and is labour intensive, which complicates the crop growth monitoring process (Liu et al. 2022b).

Few studies employed satellite platforms to estimate the AGB of potatoes (Table 4). The limited application of satellite remote sensing could be due to the low spatial and temporal resolutions of most freely available satellites. The long revisit cycles of most satellites make it difficult to obtain crop AGB data for the desired growth stages (Wan et al. 2021).

Aboveground biomass of potato has been predicted with varying accuracy ($R^2 = 0.20 – 0.90$) using different models (Table 4). Estimation of crop AGB through remote sensing is mainly performed using physical and statistical models. Physically based models for estimating AGB involve the use of radiative transfer models (RTMs), such as the PROSAIL model (Duan et al. 2014). The physical models use canopy reflectance at 400 – 2500 nm wavelengths as input (Duan et al. 2014; Weiss et al. 2020). The inversion of RTMs using canopy reflectance values from remote sensing allows the estimation of plant variables such as chlorophyll content, dry matter content, LAI, carotenoid content, and leaf equivalent water thickness (Wan et al. 2021), which are used to calculate AGB (Duan et al. 2014). Statistical models are empirical regression equations relating ground measured AGB and remotely sensed spectral features such as VIs, canopy texture variables, geometric variables, canopy height, and fractional vegetation cover (Luo et al. 2022). Statistical models employed for AGB estimation included multiple regression, partial least squares regression (PLSR) and principal component analysis (PCA) (Table 4). Recently ML techniques such as Random Forest, artificial neural network (ANN) and SVM that incorporate multiple VIs, canopy texture features and crop height have been explored for AGB estimation (Zhu et al. 2019; Li et al. 2020c; Liu et al. 2022c).

Vegetation Indices for Aboveground Biomass Monitoring

The most commonly used VIs included NDVI, optimized SAVI (OSAVI), re-normalized difference vegetation index (RDVI), and modified simple ratio (MSR) (Table 3). Most studies associated NDVI with the AGB of potato, with relationships showing varying strengths. However, NDVI is affected by reflectance from the soil surfaces, especially at low canopy cover, and has low sensitivity to AGB at high canopy cover (Xue and Su 2017). This affects the accuracy of AGB estimation using NDVI. Therefore, alternative VIs such as RDVI, SAVI, OSAVI, TSAVI, $CI_{red\text{-}edge}$, MSR among others, with the capability to distinguish between crop vegetation and soil reflectance, have been evaluated for accurate AGB estimation. Although most VIs are positively correlated with AGB (Pei et al. 2019), they tend to saturate at high vegetation cover, making them inefficient for estimating AGB at different crop

growth stages (Liu et al. 2022e). Therefore, techniques, including the use of plant height extracted from digital surface models (DSMs) (Roth and Streit 2018), microwave SAR backscatter (Gao et al. 2013; Hosseini et al. 2019), light detection and ranging (LiDAR) (Li et al. 2015; ten Harkel et al. 2020) and canopy texture features from ultrahigh ground-resolution RGB digital images have been investigated (Yue et al. 2018; Liu et al. 2022b).

Plant height is used to characterize vertical crop growth; therefore, it can be used to estimate other crop variables, including AGB (Yue et al. 2018; Lu et al. 2019). Crop AGB has been estimated using plant height extracted from DSMs and digital terrain models (Bendig et al. 2015; Mao et al. 2021). DSMs can be generated from RGB ultrahigh-ground resolution digital images using structure-from-motion algorithms (Aasen et al. 2015). Combining plant height and VIs in statistical models improves the accuracy of AGB estimation (Bendig et al. 2015; Yue et al. 2018; Lu et al. 2019), as it enables the use of both spectral and structural information (Lu et al. 2019; Niu et al. 2019). Liu et al. (2022b) found that the use of crop height and canopy texture features results in more accurate estimation of potato AGB ($R^2 = 0.73 – 0.78$) than using texture features alone ($R^2 = 0.59 – 0.73$).

Microwave SAR is sensitive to biophysical crop variables including LAI, biomass, and canopy height (Jin et al. 2015; Ndikumana et al. 2018). Synthetic aperture radar backscatter is advantageous over optical remote sensing because it can penetrate crop canopies and circumvent the premature saturation of AGB estimates, particularly during periods of full canopy coverage (Gao et al. 2013; Liu et al. 2022b). Research has demonstrated that the backscattering coefficients from SAR can accurately estimate the AGB in various crops, including wheat (Jin et al. 2015; Han et al. 2019), maize (Gao et al. 2013; Hosseini et al. 2019), rice (Ndikumana et al. 2018), and soybean (Mandal et al. 2019).

LiDAR, or laser-scanning remote sensing, involves the transmission of electromagnetic pulses (laser pulses) with a specific penetration ability to interact with vegetation and ground surfaces (Poley and McDermid 2020; Sun et al. 2022). The interaction between laser pulses and ground objects is used to characterize crop canopy structural and biophysical variables, such as volume, height, density, LAI, stem diameter, and coverage, which are useful for estimating the AGB (Jimenez-Berni et al. 2018; Poley and McDermid 2020; ten Harkel et al. 2020). For example, Li et al. (2015) demonstrated that the canopy height and LAI acquired by LiDAR correlated strongly with aboveground and belowground maize biomass. Jimenez-Berni et al. (2018) accurately ($R^2 > 0.90$) estimated the canopy height, ground cover, and biomass of wheat using a LiDAR-based 3-dimensional profile index (3DPI) model. Similarly, ten Harkel et al. (2020) evaluated the potential of a 3DPI model based on LiDAR point clouds to estimate winter wheat, sugar beet, and potato biomass. The 3DPI estimated biomass well for sugar beet ($R^2 = 0.68$) and winter wheat ($R^2 = 0.82$), but poorly estimated potato biomass ($R^2 = 0.24$). Additional research is needed to assess the potential of LiDAR technology for potato AGB estimation.

Canopy texture features such as gray scale variance, homogeneity, contrast, dissimilarity, entropy and second moment obtained from ultrahigh-ground-resolution RGB digital images provide useful information for estimating crop variables, such as LAI, plant density, chlorophyll content, nitrogen content, and AGB (Yue et al.

2018; Poley and McDermid 2020; Zhai et al. 2023). Canopy texture features have been used to accurately estimate crop AGB for rice (Zheng et al. 2019), winter wheat (Yue et al. 2019) and potato (Liu et al. 2022c, b). Studies by Li et al. (2020b) and Liu et al. (2022c) revealed that combining multiple VIs, texture features, plant height, and canopy cover improved the accuracy of potato AGB estimation.

The strength of the relationship between VIs and AGB increases from emergence to tuber bulking stages and declines from tuber bulking until crop maturity (Liu et al. 2022d). VIs are strongly associated with AGB at the tuber bulking stage ($R^2 = 0.62 – 0.92$) (Pei et al. 2019; Yang et al. 2021; Liu et al. 2022a; d). This trend can be related to the potato growth cycle, where maximum vegetative growth and full canopy cover are attained during the tuber initiation and bulking growth stages (Haverkort 2018). Therefore, the spectral information obtained between the tuber initiation and bulking stages reflected AGB relatively well (Pei et al. 2019; Liu et al. 2022d). During the later growth stages, leaves start to senesce, resulting in a reduction in canopy cover; hence, crop canopy is a poorer predictor of AGB in this stage.

Potato Leaf Area Index

Leaf area index, defined as the total one-sided area of leaf tissue per unit ground surface area, is a good indicator of vegetation status, photosynthetic rate, biomass accumulation, and evapotranspiration (Wan et al. 2021). Timely estimation of potato LAI using remote sensing has been investigated by various researchers (Table 5). Unmanned aerial vehicles equipped with hyperspectral sensors and satellites equipped with multispectral sensors were the most commonly used remote sensing platforms for potato LAI monitoring (Table 5). However, no single remote sensing platform provides images with high spectral, spatial, and temporal resolutions at a low cost. Therefore, the use of different optical sensors on various platforms has been explored for estimating potato LAI (Franceschini et al. 2017a). Ground-based sensors, such as multispectral cameras (Roosjen et al. 2018) and Cropscan multispectral radiometers (Clevers et al. 2017; Franceschini et al. 2017a), were employed to obtain ground-truth reflectance data for calibrating the UAV hyperspectral and satellite multispectral data. Gevaert et al. (2014, 2015), investigated the utility of continuous surface reflectance (spectral-temporal response surfaces, STRSs) derived from the integration of Formosat-2 multispectral satellite imagery and UAV hyperspectral imagery. The findings indicated that STRSs obtained from both satellite multispectral and UAV hyperspectral data can be employed to derive VIs for estimating potato LAI and chlorophyll content, with R^2 ranging from 0.1 – 0.84. However, studies on image fusion techniques utilizing satellite and UAV data to estimate potato LAI remain limited.

Leaf area index can be estimated from remote sensing using three approaches: biophysical processors, RTMs, and statistical models (Wan et al. 2021). The LAI can be retrieved from the biophysical processor tool of the Sentinel Application Platform (SNAP) created by the European Space Agency (Mourad et al. 2020). The SNAP software includes neural network algorithms trained to process biophysical traits such as LAI and LCC from Sentinel-2 imagery. Additionally, Mourad et al.

Table 5 Comparison of remote sensing type, models and main input features for potato leaf area index estimation

Data source	Model and input features	Prediction accuracy[a]	References
UAV_ hyper- & multi-spectral cameras	Inversion of PROSAIL model-nadir & angular data	*R^2 = 0.40–0.99	(Duan et al. 2014; Roosjen et al. 2018)
UAV_hyperspectral cameras & Ground-based Cropscan spectrometers	Regression with TCARI and LAI	*R^2 = 0.70	(Franceschini et al. 2017a)
UAV_hyperspectral & Formosat-2 satellite images	Regression & STRS methodology (OSAVI, MCARI, WDVI, LAI)	R^2 = 0.83–0.95	(Gevaert et al. 2014; 2015)
Sentinel-2 and Venus satellites_multispectral sensors	PLSR_ REIP and NDVI and LAI	*R^2 = 0.60–62	(Herrmann et al. 2011)
Landsat-8 and Sentinel-2_multispectral sensors	Regression analysis with EVI2, SAVI	R^2 = 0.59	(Mourad et al. 2020)
QuickBird satellite_multispectral sensors	Regression_ NDVI, SAVI, MSAVI, TSAVI and PVI	R^2 = 0.89	(Wu et al. 2007)
Sentinel-2 satellite & Cropscan radiometer	Regression_Multiple VIs	R^2 = 0.81	(Clevers et al. 2017)
Ground-based Field spectroradiometer	Regression & PCA_VIs	*R^2 = 0.80–0.94	(Ray et al. 2006; Nguy-Robertson et al. 2014)

UAV is unmanned aerial vehicle, *VIs* is vegetation indices, *NDVI* is normalized difference vegetation index, *LAI* is leaf area index, *STRS* is spectral-temporal response surfaces, *TCARI* is transformed chlorophyll in reflectance index, *MCARI* is modified chlorophyll absorption in reflectance index, *SAVI* is soil-adjusted vegetation index, *OSAVI* is optimized SAVI, MSAVI is modified SAVI, *TSAVI* is transformed SAVI, *WDVI* is weighted difference vegetation index, *REIP* is red-edge inflection point, *EVI2* is enhanced vegetation index 2, *PSLR* is partial least squares regression and *PCA* is principal component analysis. [a]Note: the R^2 values with an asterisk (*R^2) indicate the total variance explained by multiple variables, including VIs and non-remote sensing features in a predictive model

(2020) indicated that the SNAP biophysical processor tool underestimated the LAI for various crops, including potato ($R^2 = 0.27$), compared to VI-based statistical models ($R^2 = 0.51 - 0.63$). However, additional research is needed to fully assess the dependability of the SNAP biophysical processor in estimating the LAI of crops.

The PROSAIL model, which integrates the PROSPECT and SAIL models, is the most commonly used RTM for simulating crop canopy reflectance as a function of LAI, leaf angle distribution function, chlorophyll content, dry matter content, carotenoid content, leaf equivalent water thickness, canopy reflectance background, sensor viewing angle, sun zenith, and azimuth angles (Roosjen et al. 2018; Wan et al. 2021). To retrieve LAI using RTMs, model inversion techniques such as iterative optimization, look-up tables, and neural networks must be applied (Duan et al. 2014; Verrelst et al. 2015). A specific set of model parameter values that result in simulated canopy reflectance similar to remote sensing canopy reflectance is utilized to estimate the LAI. Duan et al. (2014) assessed the capacity of the PROSAIL model to estimate LAI for maize, potato, and sunflower using UAV hyperspectral data. The results indicated that the model accurately simulated LAI for all three crops, with root mean square error ranging from 0.55 – 0.60 m^2 m^{-2}. However, differences were observed between the model-estimated and ground measured LAI values, which were attributed to the inability of the model to account for the shading effect of row crops. The shading effect can lead to an enhancement or reduction in crop canopy reflectance, depending on the UAV flight direction (Duan et al. 2014).

Statistical models are based on established empirical relationships between VIs and ground-measured LAI using devices such as a Plant Canopy Analyzer (LAI-2000, LI-COR), AccuPAR LP-80 ceptometer, and LI-3100C leaf area meter (Clevers et al. 2017). These empirical relationships can take various forms, including linear, exponential, logarithmic polynomial, and inverse exponential expressions (Ray et al. 2006). Haboudane et al. (2004) and Ray et al. (2006) found that exponential relationships between LAI of various crops and VIs had the highest R^2 values compared to linear, power, and logarithmic relationships. This may be because indices based on the ratio or product of red and NIR wavelengths are highly sensitive to chlorophyll content and tend to saturate at LAI greater than 3 m^2 m^{-2} (Haboudane et al. 2004). Although statistical models are simple to compute, they require extensive calibration and validation using ground truth data (Mourad et al. 2020). Moreover, these models are limited to a specific set of conditions, such as crop type, crop management, weather, and soil conditions, under which they are created, which restricts their use in different conditions. Despite these limitations, statistical models are the most frequently used for estimating the potato LAI, with the relationship between LAI and VIs showing varying R^2 ranging from 0.52 – 0.95 (Table 5).

The accuracy (indicated by R^2) of LAI estimations, regardless of the model used, ranged between 0.40 – 0.99, which suggests that remote sensing data can be used to estimate the LAI of potato with considerable accuracy (Table 5). The most popular indices for potato LAI estimation included NDVI, SAVI, WDVI, red-edge NDVI, red-edge inflection point (REIP) and GNDVI (Table 3). Reflectance in the green, red and NIR regions is directly related to the LAI, greenness, and canopy cover (Hermann et al. 2011). However, indices based on NIR and red bands, such as NDVI and RVI, tended to be less sensitive to LAI greater than 2 m^2 m^{-2}, whereas indices

combining green and red-edge bands were highly sensitive to LAI above 4 m^2 m^{-2} (Gitelson 2004; Herrmann et al. 2011). In addition, reflectance in the NIR region tended to be affected by soil reflectance, particularly during the early crop stages (Morier et al. 2015). To eliminate the effects of the soil background, VIs such as the WDVI, wide dynamic range vegetation index (WDRVI), SAVI, and OSAVI were created with a soil reflectance correction factor in the NIR region, which improved their sensitivity to LAI (Huete 1988; Clevers 1989; Haboudane et al. 2002; Gitelson 2004). Although VIs with minimal interference from soil background reflectance are highly sensitive to LAI, there is currently no specific VI for LAI estimation. Furthermore, the dependence of spectral reflectance in the visible and NIR regions on both LAI and chlorophyll content makes it challenging to find a VI that is not influenced by the chlorophyll content. Haboudane et al. (2004), proposed the MCARI2 and the modified triangular vegetation index 2 (MTVI2), which are highly sensitive to changes in LAI and have low sensitivity to chlorophyll content. Therefore, future research should investigate the nature of the relationship between MCARI2, MTVI2, and potato LAI.

Few studies evaluated the relationship between the VIs and LAI of potato at different growth stages. Clevers et al. (2017) evaluated the temporal pattern of WDVI as an estimator of LAI of potato during the season. The R^2 values between the WDVI and LAI of potato at 52, 85, 95, and 122 DAP were 0.71, 0.92, 0.87, and 0.92, respectively (Clevers et al. 2017). More research is needed to determine the most suitable time to estimate the LAI using VIs.

Estimating Potato Leaf and Canopy Chlorophyll Content

Leaf chlorophyll content (LCC) and canopy chlorophyll content (CCC) serve as indicators of crop physiological status, health, nutritional status, and productivity (Evans 1989; Elarab et al. 2015). Leaf chlorophyll content is closely related to leaf N, and can therefore be used as an indicator for N nutrition in leaves to guide fertilizer application in potatoes (Evans 1989; Clevers et al. 1994; van Evert et al. 2012). Therefore, timely and accurate estimation of chlorophyll content can aid in the implementation of crop management interventions for potatoes, leading to improved crop growth and optimized yield. Traditional methods for estimating chlorophyll content involve laboratory techniques such as liquid chromatography, atomic absorption, and spectrophotometry (Li et al. 2020b). These methods require destructive leaf sampling, which is time-consuming and laborious. Traditional methods are limited to small areas, necessitating the use of remote sensing techniques for real-time chlorophyll estimation over relatively large areas (Gao et al. 2021). Research has shown that reflectance in specific portions of the spectrum between the visible and NIR regions is sensitive to chlorophyll content. Vegetation indices based on reflectance in the green, red-edge and NIR bands are strongly correlated with LCC and CCC (Gitelson and Merzlyak 1996; Borhan et al. 2017).

The remote sensing platforms, sensors, and models used for estimating LCC and CCC of potato are listed in Table 6. UAVs equipped with multispectral and hyperspectral sensors, and ground-based (handheld) devices such as the Field

Table 6 Comparison of remote sensing models and main input features used for potato leaf and canopy chlorophyll estimation

Data source	Models and features	Prediction accuracy[a]	References
UAV with hyperspectral cameras	Regression & ML_Multiple VIs & full spectrum	*R^2 = 0.86	(Li et al. 2020a; 2021a)
UAV with multispectral sensors	ML with Recursive feature elimination & PCA_ Multiple VI, texture features	*R^2 = 0.69–0.76	(Yang et al. 2022; Yin et al. 2022)
UAV-hyperspectral sensors and Handheld Cropscan multispectral radiometer	Regression_Multiple VIs	R^2 = 0.63–0.73	(Franceschini et al.; 2017a)
Handheld Camera, Fieldspec & Cropscan radiometers	Regression_green and blue image features, PROSAIL model _spectral bands & multiple VIs	*R^2 = 0.80–0.94	(Kooistra and Clevers 2016; Borhan et al. 2017)
Handheld Digital camera	Regression & ANN_Image analysis of RGB Features	R^2 = 0.59–0.80	(Gupta et al. 2013) (Yadav et al. 2010)
Handheld Cropscan radiometer & RapidEye satellites	Regression and PROSAIL model _Multiple VIs	*R^2 = 0.94	(Kooistra and Clevers 2016)
Satellite Sentinel-2_Multispectral sensors	Regression_Multiple VIs	R^2 = 0.81	(Clevers et al. 2017)
Satellite Formosat-2 & UAV_Multispectral sensors	STRSs with Bayesian theory_Multiple VIs	R^2 = 0.59 & 0.77	(Gevaert et al. 2014, 2015)

UAV is unmanned aerial vehicle, *VIs* is vegetation indices, *ML* is machine learning, *RGB* is red–green–blue image, *PCA* is principal component analysis, *ANN* is artificial neural network and *STRSs* is spectral-temporal response surfaces. [a]Note: the R^2 values with an asterisk (*R^2) indicate the total variance explained by multiple variables, including VIs and non-remote sensing features in a predictive model

spectrometer, Cropscan multispectral radiometers, charged-coupled devices (CCD) digital RGB cameras and the soil plant analysis development (SPAD) chlorophyll meter were the most used platforms, whereas a few studies used satellite multispectral platforms for potato LCC and CCC estimation (Table 6).

Ground-based sensors are quick, easy to operate and provide LCC and CCC estimates that can be used for ground truthing UAV and satellite-based estimations. Various regression techniques, including linear, exponential, logarithmic, multiple linear regression, and PLSR, as well as non-linear regression methods, such as ANN and Random Forest, have been employed to establish LCC and CCC prediction models. Relationships between the ground-measured chlorophyll content of potato with SPAD chlorophyll meter readings (Uddling et al. 2007), CCD digital image features, such as mean gray values, spectral luminosity, and mean brightness ratios (Yadav et al. 2010; Gupta et al. 2013; Borhan et al. 2017), and VIs derived from Cropscan radiometer reflectance measurements (Kooistra and Clevers 2016) have been established. Borhan et al. (2017) used simple linear and multiple linear regressions to show that the mean gray values of CCD digital images at 550 nm and 700 nm exhibited strong correlations with the SPAD chlorophyll meter readings of potato. Gupta et al. (2013) applied linear regression and ANN to relate the mean brightness ratios of CCD RGB images of leaves with the chlorophyll content of micropropagated potato plants. The ANN model demonstrated a higher accuracy in predicting the LCC ($R^2 = 0.82$) than simple linear regression ($R^2 = 0.59$). Kooistra and Clevers (2016) found that VIs based on Cropscan reflectance values of potato crops were linearly related to SPAD chlorophyll meter readings with an R^2 ranging from 0.43 – 0.64. In the same study, the PROSAIL model estimated chlorophyll content well ($R^2 > 0.72$) (Kooistra and Clevers 2016). Although some studies have shown promising results for the estimation of potato chlorophyll content using SPAD chlorophyll meter and CCD digital cameras, environmental factors such as nutrient deficiency, leaf disease infection, and the inherent light scattering properties of leaves can impact the accuracy of these estimates (Borhan et al. 2017). Additionally, the non-homogeneous distribution of chlorophyll within the leaves can affect the estimated chlorophyll concentration (Borhan et al. 2017).

The use of UAVs' spectral information was employed to derive VIs for establishing potato chlorophyll content estimation models (Table 6). Yin et al. (2022) implemented twelve VIs derived from UAV multispectral images as inputs for ML algorithms, including Random Forest, Support Vector Regression (SVR), PLSR, and Ridge Regression, to predict potato chlorophyll content. The findings indicated that the Random Forest model demonstrated the highest accuracy in predicting chlorophyll content, with a R^2 value of 0.76, followed by the SVR model, with a R^2 value of 0.74. Li et al. (2020b) reported that VIs derived from UAV hyperspectral data showed a strong correlation with potato chlorophyll content at all growth stages, with R^2 values ranging from 0.53 – 0.77. Additionally, the original spectrum, fractional differential spectra, spectral position, and spectral area parameters of potato reflectance were used to establish potato chlorophyll prediction models. The study conducted by Li et al. (2021a) established linear and nonlinear relationships between fractional differentiation of the canopy spectrum and chlorophyll content in potato plants at various growth stages. The R^2 for the relationship between different

fractional differentiation spectra orders and chlorophyll content ranged from 0.65 – 0.85 (Li et al. 2021a). In a separate study, Li et al. (2020b) utilized ML algorithms in conjunction with UAV hyperspectral VIs and spectral characteristics based on spectral position and spectral area to estimate the chlorophyll content in potato plants at different growth stages. The stepwise regression model demonstrated the highest prediction accuracy (R^2 ranging from 0.52 – 0.78) at all growth stages.

Most studies used $CI_{red\text{-}edge}$, CI_{green}, NDVI, and OSAVI to estimate the LCC and CCC of potato (Table 3). In addition, indices such as OSAVI (TCI/OSAVI), TCARI/OSAVI, DVI, and RVI have been strongly associated with the LCC and CCC of potatoes (Kooistra and Clevers 2016). Chlorophyll estimation requires VIs that are highly sensitive to chlorophyll concentration, resistant to variations in LAI, and unaffected by background soil reflectance (Clevers et al. 2017). These indices combine the bands of minimum chlorophyll absorption (550 nm and 700 nm) and maximum chlorophyll absorption (670 nm) (Haboudane et al. 2002). This idea led to the generation of ratio indices such as TCARI/OSAVI and MCARI/OSAVI (Gitelson and Merzlyak 1996; Haboudane et al. 2002). In addition, reflectance in the green- and red-edge regions was found to be highly sensitive to chlorophyll content (Gitelson et al. 2003). Therefore, VIs based on red-edge properties, such as red-edge position (REP), $CI_{red\text{-}edge}$, CI_{green}, CVI, and MERIS terrestrial chlorophyll index (MTCI), have been recommended for chlorophyll content estimation (Gitelson et al. 2003; Clevers et al. 2017).

As expected, chlorophyll content showed the strongest correlation with spectral features during the vegetative growth stage, with an R^2 value of 0.85. This relationship was followed by tuber initiation ($R^2 = 0.70$), tuber bulking stage ($R^2 = 0.69$), and maturation stages ($R^2 = 0.54$) (Li et al. 2020b). This finding was consistent with the use of fractional differentiation spectra orders, which produced an R^2 of 0.85 during the vegetative stage, followed by an R^2 of 0.79 at tuber initiation, an R^2 of 0.71 at tuber bulking, and an R^2 of 0.72 at starch maturation (Li et al. 2021a). Leaf greenness, leaf N content, and chlorophyll concentration are highest during the vegetative growth stage, and they gradually decline as the season progresses until crop senescence, when leaf colour changes from dark green to yellow (Borhan et al. 2017; Clevers et al. 2017; Li et al. 2020b). It is important to note that this decline in leaf greenness is a natural part of crop growth and development. Changes in the structure and biochemical components of leaves during the growing season affect spectral reflectance. Consequently, the vegetative growth period, including tuber bulking stage, is the most appropriate time for estimating chlorophyll content of potato.

Estimating Potato Leaf Nitrogen Status

Ground-based platforms were most commonly used to estimate the N status of potato leaves (Table 7). These included sensors such as Cropscan, Rapidscan, NIR analyzers, shortwave-infrared (SWIR) cameras, and SPAD meters. A possible reason for the high usage of ground-based sensors could be their high spatial resolution and the opportunities they offer for accurate ground-truth calibration. Moreover, handheld sensors are portable, facilitate measurements in small research fields, and

Table 7 Comparison of the remote sensing models used for estimating the N concentration of potato leaves and their main input features

Data source	Model and features	Most accurate model[a]	Reference
Handheld NIR analyzer	Regression_wavebands	$R^2 = 0.59$	(Abukmeil et al. 2022)
Handheld Field Spectrometer	Discriminant canonical variable_Fluorence and reflectance indices	CND-NII accuracy of 70–90%	(Bélanger et al. 2005)
Handheld mini-Spectrometer	PLSR & MLR_whole spectrum &TCARI	$*R^2 = 0.95$	(Cohen et al. 2010)
Handheld Field Spectrometer	Regression_VI and SWIR-based NIs	$R^2 = 0.52–0.55$	(Herrmann et al. 2010)
Handheld HySpex VNIR-1800 and SWIR-384 cameras	OLSR and PLSR_VI, full spectrum, SWIR	$*R^2 = 0.68–0.82$	(Liu et al. 2021)
Handheld Spectrometer	Regression and UAV_hyperspectral VIs	$R^2 = 0.72$	(Morier et al. 2015)
Handheld 512-Channel spectroradiometer	Band-band_r^2, PCA, discriminant analysis and regression_VI	$*R^2 = 0.55$	(Jain et al. 2007)
Handheld Rapidscan, UAV & Satellite-Sentinel-2	Parametric regression and RF	$*R^2 = 0.85$	(Peng et al. 2021a)
Handheld multispectral sensor	Regression_WDVI	Mean N saving of 56 kg N ha^{-1}	(van Evert et al. 2012)
Handheld Rapidscan	Regression _LAI, GCC, and VIs vs leaf N%	$R^2 = 0.78$	(Zhou et al. 2017a; 2018)
UAV-Hyperspectral Camera	Regression _VIs	$R^2 = 0.68–0.79$	(Nigon et al. 2014; 2015)
UAV-Hyperspectral Camera	PLSR _Full spectrum	$*R^2 = 0.78–0.87$	(Zhou et al. 2022)

UAV is unmanned aerial vehicle, *VIs* is vegetation indices, *VIs* is vegetation indices, *ML* is machine learning, *PLSR* is partial least square regression, multiple linear regression *MLR*, *TCARI* transformed chlorophyll absorption in reflectance index, *PCA* is principal component analysis, *RF* is random forest, *WDVI* is weighted difference vegetation index, *LAI* is leaf area index, *GCC* is ground canopy cover, *N* is nitrogen, *NIs* is nitrogen indices and *CND_NII* is compositional nutrient diagnosis nutrient imbalance index. [a]Note: the R^2 values with an asterisk ($*R^2$) indicate the total variance explained by multiple variables, including VIs and non-remote sensing features in a predictive model

have low operational costs compared with UAVs and satellites. The R^2 values for all models combined for estimating leaf/petiole N concentrations ranged from 0.52 – 0.95, suggesting that remote sensing has the potential to estimate the N status of potato with considerable accuracy (Table 7).

The most commonly used indices were NDVI, MCARI, TCARI, and TCARI/OSAVI ratio (Table 3). Cohen et al. (2010) evaluated the relationship between TCARI and potato leaf N levels, and they found that TCARI is strongly associated with leaf N% and petiole NO_3-N only at the tuber bulking stage ($R^2 = 0.80$ and 0.76). Goffart et al. (2022) showed that the best linear and Random Forest models for estimating shoot N concentration and N uptake of potato were those combining the TCARI/OSAVI, WDVI, $CI_{red\text{-}edge}$, and RVI indices. Jain et al. (2007) showed that the ratio of reflectance at red-edge bands 750 nm and 710 nm (RRE,750/710) is strongly associated with leaf N content of potato between 40 – 60 DAP. Peng et al. (2021a) suggested that the RVI, NDRE, and transformed chlorophyll index (TCI) were the most suitable indices for estimating the NNI of potato. Based on the above analysis, there is substantial variation in opinions regarding the most suitable VIs for estimating potato N status; however, red-edge-based indices appear to be the most suitable. This suggests that more research is required to confirm the suitability of red-edge indices for potato N status estimation.

Conclusions

- Satellite images were the most widely used source of remote sensing data for potato yield prediction, whereas UAVs and handheld sensors were most widely used for potato growth monitoring.
- A combination of regression analysis and ML models was used to generate prediction models for all aspects of potato growth and yield, with VIs and spectral bands as the main features. The most common VIs for the yield prediction models were the NDVI, $CI_{red\text{-}edge}$, OSAVI, and CI_{green}.
- Strong associations between tuber yield and NDVI, EVI, NDRE, and $CI_{red\text{-}edge}$, suggested that these indices are most appropriate for estimating tuber yield. A strong association was also reported between potato LAI and NDVI, OSAVI, WDVI, and GNDVI.
- The chlorophyll content of potato correlated well with CI_{green}, $CI_{red\text{-}edge}$, TCI/OSAVI, and TCARI/OSAVI. However, combining multiple VIs with original canopy spectrum measurements using PLSR resulted in improved chlorophyll content estimation. Indices calculated from red-edge bands, such as the $CI_{red\text{-}edge}$, NDRE, and red-edge 740/720 indices, were strongly associated with leaf N concentration.
- Most studies reported that VIs have a weak association with potato AGB because they tend to saturate at high vegetation cover. Accurate AGB estimation can be achieved by combining multiple VIs, plant height, canopy cover, and the original canopy spectrum in ML models.

- Vegetation indices acquired during maximum ground cover and tuber initiation, (approximately 36 – 55 DAP) were strongly associated with potato growth variables and final tuber yield.
- The findings of this systematic review should be helpful in informing researchers, agronomists and farmers about the most suitable VIs and the most appropriate time for using remote sensing for potato growth monitoring and tuber yield prediction.

Funding Open access funding provided by University of Pretoria.

Data Availability The data collected for this paper can be obtained from the corresponding author upon request.

Declarations

Ethical Statement No ethics have been violated in compiling this article.

Conflicts of Interest The corresponding author is an editorial board member of Potato Research.

References

Aasen H, Burkart A, Bolten A, Bareth G (2015) Generating 3D hyperspectral information with lightweight UAV snapshot cameras for vegetation monitoring: From camera calibration to quality assurance. ISPRS J Photogramm Remote Sens 108:245–259. https://doi.org/10.1016/j.isprsjprs.2015.08.002

Abbas F, Afzaal H, Farooque AA, Tang S (2020) Crop yield prediction through proximal sensing and machine learning algorithms. Agronomy 10:2–16. https://doi.org/10.3390/AGRONOMY10071046

Abdikan S, Sekertekin A, Ustunern M, Sanli FB, Nasirzadehdizaji R (2018) Backscatter analysis using multi-temporal Sentinel-1 SAR data for crop growth of maize in Konya Basin, Turkey. Int Arch Photogramm Remote Sens Spatial Inf Sci 42:9–13

Abou Ali H, Delparte D, Griffel LM (2020) From pixel to yield: Forecasting potato productivity in Lebanon and Idaho. International Archives of the Photogrammetry. Remote Sensing and Spatial Information Sciences - ISPRS Archives. Maryland, USA, pp 1–7

Abrougui K, Gabsi K, Mercatoris B, Khemis C, Amami R, Chehaibi S (2019) Prediction of organic potato yield using tillage systems and soil properties by artificial neural network (ANN) and multiple linear regressions (MLR). Soil Tillage Res 190:202–208. https://doi.org/10.1016/j.still.2019.01.011

Abukmeil R, Al-Mallahi AA, Campelo F (2022) New approach to estimate macro and micronutrients in potato plants based on foliar spectral reflectance. Comput Electron Agric 198:107074–107097. https://doi.org/10.1016/j.compag.2022.107074

Ahmad U, Alvino A, Marino S (2021) A review of crop water stress assessment using remote sensing. Remote Sens 13:4155

Al-Gaadi KA, Hassaballa AA, Tola E, Kayad AG, Madugundu R, Alblewi B, Assiri F (2016) Prediction of potato crop yield using precision agriculture techniques. PLoS ONE 11:1–16. https://doi.org/10.1371/journal.pone.0162219

Allen R, Irmak A, Trezza R, Hendrickx JMH, Bastiaanssen W, Kjaersgaard J (2011) Satellite-based ET estimation in agriculture using SEBAL and METRIC. Hydrol Process 25:4011–4027. https://doi.org/10.1002/hyp.8408

Allen RG, Tasumi M, Morse A (2005) Satellite-based evapotranspiration by METRIC and Landsat for western states water management. Presented at the US Bureau of Reclamation Evapotranspiration Workshop, Ft. Collins, CO, USA

Arslan İ, Topakcı M, Demir N (2022) Monitoring maize growth and calculating plant heights with synthetic aperture radar (SAR) and optical satellite images. Agric 12:800. https://doi.org/10.3390/agriculture12060800

Aryalekshmi BN, Biradar RC, Chandrasekar K, Mohammed Ahamed J (2021) Analysis of various surface energy balance models for evapotranspiration estimation using satellite data. Egypt J Remote Sens Sp Sci 24:1119–1126. https://doi.org/10.1016/j.ejrs.2021.11.007

Awad MM (2019) Toward precision in crop yield estimation using remote sensing and optimization techniques. Agric 9:1–13. https://doi.org/10.3390/agriculture9030054

Bala SK, Islam AS (2009) Correlation between potato yield and MODIS-derived vegetation indices. Int J Remote Sens 30:2491–2507. https://doi.org/10.1080/01431160802552744

Bashir MA, Hata T, Tanakamaru H, Abdelhadi AW, Tada A (2008) Satellite-based energy balance model to estimate seasonal evapotranspiration for irrigated sorghum: A case study from the Gezira scheme, Sudan. Hydrol Earth Syst Sci 12:1129–1139. https://doi.org/10.5194/hess-12-1129-2008

Basso B, Liu L (2019) Seasonal crop yield forecast: Methods, applications, and accuracies. Adv Agron 154:201–255

Basso B, Cammarano D, Carfagna E (2013) Review of crop yield forecasting methods and early warning systems. In Proceedings of the first meeting of the scientific advisory committee of the global strategy to improve agricultural and rural statistics (Vol. 241). FAO Headquarters, Rome, Italy

Bastiaanssen WGM, Menenti M, Feddes RA, Holtslag AAM (1998) A remote sensing surface energy balance algorithm for land (SEBAL): 1. Formulation J Hydrol 212–213:213–229. https://doi.org/10.1016/S0022-1694(98)00254-6

Bastiaanssen WGM, Noordman EJM, Pelgrum H, Davids G, Thoreson BP, Allen RG (2005) SEBAL model with remotely sensed data to improve water-resources management under actual field conditions. J Irrig Drain Eng 131:85–93. https://doi.org/10.1061/(asce)0733-9437(2005)131:1(85)

Basu S, Groot SPC (2023) Seed vigour and invigoration. In: Dadlani M, Yadav DK (eds) Seed Science and Technology: Biology, Production, Quality, 1st edn. Springer Nature Singapore Pte Ltd., New Delhi, India, pp 67–91

Bélanger MC, Viau AA, Samson G, Chamberland M (2005) Determination of a multivariate indicator of nitrogen imbalance (MINI) in potato using reflectance and fluorescence spectroscopy. Agron J 97:1515–1523. https://doi.org/10.2134/agronj2005.0040

Bendig J, Yu K, Aasen H, Bolten A, Bennertz S, Broscheit J, Gnyp ML, Bareth G (2015) Combining UAV-based plant height from crop surface models, visible, and near infrared vegetation indices for biomass monitoring in barley. Int J Appl Earth Obs Geoinf 39:79–87. https://doi.org/10.1016/j.jag.2015.02.012

Boote KJ, Jones JW, Pickering NB (1996) Potential uses and limitations of crop models. Agron J 88:704–716. https://doi.org/10.2134/agronj1996.00021962008800050005x

Borhan MS, Panigrahi S, Satter MA, Gu H (2017) Evaluation of computer imaging technique for predicting the SPAD readings in potato leaves. Inf Process Agric 4:275–282. https://doi.org/10.1016/j.inpa.2017.07.005

Bouman BAM, van Kasteren HWJ (1990) Ground-based X-band (3-cm wave) radar backscattering of agricultural crops. I. Sugar beet and potato; backscattering and crop growth. Remote Sens Environ 34:93–105. https://doi.org/10.1016/0034-4257(90)90101-Q

Campos I, Neale CMU, Suyker AE, Arkebauer TJ, Goncalves IZ (2017) Reflectance-based crop coefficients REDUX: For operational evapotranspiration estimates in the age of high producing hybrid varieties. Agric Water Manag 187:140–153. https://doi.org/10.1016/j.agwat.2017.03.022

Choudhury BJ, Ahmed NU, Idso SB, Reginato RJ, Daughtry CST (1994) Relations between evaporation coefficients and vegetation indices studied by model simulations. Remote Sens Environ 50:1–17. https://doi.org/10.1016/0034-4257(94)90090-6

Clevers JGPW (1989) Application of a weighted infrared-red vegetation index for estimating leaf area index by correcting for soil moisture. Remote Sens Environ 29:25–37. https://doi.org/10.1016/0034-4257(89)90076-X

Clevers JGPW, Kooistra L (2012) Using hyperspectral remote sensing data for retrieving canopy chlorophyll and nitrogen content. IEEE J Sel Top Appl Earth Obs Remote Sens 5:574–583. https://doi.org/10.1109/JSTARS.2011.2176468

Clevers JGPW, van Leeuwen HJC (1996) Combined use of optical and microwave remote sensing data for crop growth monitoring. Remote Sens Environ 56:42–51. https://doi.org/10.1016/0034-4257(95)00227-8

Clevers JGPW, Büker C, van Leeuwen HJC, Bouman BAM (1994) A framework for monitoring crop growth by combining directional and spectral remote sensing information. Remote Sens Environ 50:161–170. https://doi.org/10.1016/0034-4257(94)90042-6

Clevers JGPW, Kooistra L, van den Brande MMM (2017) Using Sentinel-2 data for retrieving LAI and leaf and canopy chlorophyll content of a potato crop. Remote Sens 9:1–15. https://doi.org/10.3390/rs9050405

Cohen Y, Alchanatis V, Zusman Y, Dar Z, Bonfil DJ, Karniel A, Zilberman A, Moulin A, Ostrovsky V, Levi A, Brikman R, Shenker M (2010) Leaf nitrogen estimation in potato based on spectral data and on simulated bands of the VENμS satellite. Precis Agric 11:520–537. https://doi.org/10.1007/s11119-009-9147-8

Couture JJ, Singh A, Charkowski AO, Groves RL, Gray SM, Bethke PC, Townsend PA (2018) Integrating spectroscopy with potato disease management. Plant Dis 102:2233–2240. https://doi.org/10.1094/pdis-01-18-0054-re

Craufurd PQ, Vadez V, Jagadish SVK, Prasad PVV, Zaman-Allah M (2013) Crop science experiments designed to inform crop modeling. Agric for Meteorol 170:8–18. https://doi.org/10.1016/j.agrformet.2011.09.003

Cucho-Padin G, Rinza J, Ninanya J, Loayza H, Quiroz R, Ramirez DA (2020) Development of an open-source thermal image processing software for improving irrigation management in potato crops (Solanum tuberosum L.). Sensors (switzerland) 20:1–17. https://doi.org/10.3390/s20020472

Delegido J, Fernandez G, Gandia S, Moreno J (2008) Retrieval of chlorophyll content and LAI of crops using hyperspectral techniques: Application to PROBA/CHRIS data. Int J Remote Sens 29:7107–7127. https://doi.org/10.1080/01431160802238401

Dente L, Satalino G, Mattia F, Rinaldi M (2008) Assimilation of leaf area index derived from ASAR and MERIS data into CERES-Wheat model to map wheat yield. Remote Sens Environ 112:1395–1407. https://doi.org/10.1016/j.rse.2007.05.023

Doraiswamy PC, Moulin S, Cook PW, Stern A (2003) Crop yield assessment from remote sensing. Photogramm Eng & Remote Sens 69:665–674. https://doi.org/10.14358/PERS.69.6.665

Duan SB, Li ZL, Wu H et al (2014) Inversion of the PROSAIL model to estimate leaf area index of maize, potato, and sunflower fields from unmanned aerial vehicle hyperspectral data. Int J Appl Earth Obs Geoinf 26:12–20. https://doi.org/10.1016/j.jag.2013.05.007

Duarte-Carvajalino JM, Alzate DF, Ramirez AA et al (2018) Evaluating late blight severity in potato crops using unmanned aerial vehicles and machine learning algorithms. Remote Sens 10:1513. https://doi.org/10.3390/rs10101513

Duchemin B, Hadria R, Erraki S et al (2006) Monitoring wheat phenology and irrigation in Central Morocco: On the use of relationships between evapotranspiration, crops coefficients, leaf area index and remotely-sensed vegetation indices. Agric Water Manag 79:1–27. https://doi.org/10.1016/j.agwat.2005.02.013

Elarab M, Ticlavilca AM, Torres-Rua AF et al (2015) Estimating chlorophyll with thermal and broadband multispectral high resolution imagery from an unmanned aerial system using relevance vector machines for precision agriculture. Int J Appl Earth Obs Geoinf 43:32–42. https://doi.org/10.1016/j.jag.2015.03.017

Elsayed S, El-Hendawy S, Khadr M et al (2021a) Integration of spectral reflectance indices and adaptive neuro-fuzzy inference system for assessing the growth performance and yield of potato under different drip irrigation regimes. Chemosensors 9:1–25. https://doi.org/10.3390/chemosensors9030055

Elsayed S, El-Hendawy S, Khadr M et al (2021b) Combining thermal and rgb imaging indices with multivariate and data-driven modeling to estimate the growth, water status, and yield of potato under different drip irrigation regimes. Remote Sens 13:1–28. https://doi.org/10.3390/rs13091679

Evans JR (1989) Photosynthesis and nitrogen relationships in leaves of C3 plants. Oecologia 78:9–19. https://doi.org/10.1109/LSP.2017.2723724

Franceschini MHD, Bartholomeus H, van Apeldoorn D et al (2017a) Intercomparison of unmanned aerial vehicle and ground-based narrow band spectrometers applied to crop trait monitoring in organic potato production. Sensors (Switzerland) 17:1–36. https://doi.org/10.3390/s17061428

Franceschini MHD, Bartholomeus H, Van Apeldoorn D et al (2017b) Assessing changes in potato canopy caused by late blight in organic production systems through UAV-based pushbroom imaging spectrometer. Int Arch Photogramm Remote Sens Spat Inf Sci - ISPRS Arch 42:109–112. https://doi.org/10.5194/isprs-archives-XLII-2-W6-109-2017

Franceschini MHD, Bartholomeus H, van Apeldoorn DF et al (2019) Feasibility of unmanned aerial vehicle optical imagery for early detection and severity assessment of late blight in Potato. Remote Sens 11:224. https://doi.org/10.3390/rs11030224

Gao S, Niu Z, Huang N, Hou X (2013) Estimating the leaf area index, height and biomass of maize using HJ-1 and RADARSAT-2. Int J Appl Earth Obs Geoinf 24:1–8. https://doi.org/10.1016/j.jag.2013.02.002

Gao D, Li M, Zhang J et al (2021) Improvement of chlorophyll content estimation on maize leaf by vein removal in hyperspectral image. Comput Electron Agric 184:106077. https://doi.org/10.1016/j.compag.2021.106077

Gerhards M, Rock G, Schlerf M, Udelhoven T (2016) Water stress detection in potato plants using leaf temperature, emissivity, and reflectance. Int J Appl Earth Obs Geoinf 53:27–39. https://doi.org/10.1016/j.jag.2016.08.004

Gevaert CM, Suomalainen J, Tang J, Kooistra L (2015) Generation of spectral-temporal response surfaces by combining multispectral satellite and hyperspectral UAV imagery for precision agriculture applications. IEEE J Sel Top Appl Earth Obs Remote Sens 8:3140–3146. https://doi.org/10.1109/JSTARS.2015.2406339

Gevaert CM, Tang J, Garcia-Haro FJ et al (2014) Combining hyperspectral UAV and multispectral Formosat-2 imagery for precision agriculture applications. In 2014 6th Workshop on Hyperspectral Image and Signal Processing: Evolution in Remote Sensing (WHISPERS). IEEE Lausanne, Switzerland, pp 1–4

Gitelson AA (2004) Wide dynamic range vegetation index for remote quantification of biophysical characteristics of vegetation. J Plant Physiol 161:165–173

Gitelson AA, Merzlyak MN (1996) Signature analysis of leaf reflectance spectra: Algorithm development for remote sensing of chlorophyll. J Plant Physiol 148:494–500. https://doi.org/10.1016/S0176-1617(96)80284-7

Gitelson AA, Gritz Y, Merzlyak MN (2003) Relationships between leaf chlorophyll content and spectral reflectance and algorithms for non-destructive chlorophyll assessment in higher plant leaves. J Plant Physiol 160:271–282. https://doi.org/10.1078/0176-1617-00887

Glenn EP, Nagler PL, Huete AR (2010) Vegetation index methods for estimating evapotranspiration by remote sensing. Surv Geophys 31:531–555. https://doi.org/10.1007/s10712-010-9102-2

Gnyp ML, Miao Y, Yuan F et al (2014) Hyperspectral canopy sensing of paddy rice aboveground biomass at different growth stages. F Crop Res 155:42–55. https://doi.org/10.1016/j.fcr.2013.09.023

Goffart D, Ben AF, Curnel Y et al (2022) In-season potato crop nitrogen status assessment from satellite and meteorological data. Potato Res 65:729–755. https://doi.org/10.1007/s11540-022-09545-0

Gold KM, Townsend PA, Herrmann I, Gevens AJ (2020) Investigating potato late blight physiological differences across potato cultivars with spectroscopy and machine learning. Plant Sci 295:110316–110328. https://doi.org/10.1016/j.plantsci.2019.110316

Gomez D, Salvador P, Sanz J, Casanova JL (2019) Potato yield prediction using machine learning techniques and Sentinel 2 data. Remote Sens 11:1–17

Gómez D, Salvador P, Sanz J, Casanova JL (2021) New spectral indicator Potato Productivity Index based on Sentinel-2 data to improve potato yield prediction: a machine learning approach. Int J Remote Sens 42:3430–3448. https://doi.org/10.1080/01431161.2020.1871102

González-Dugo MP, Mateos L (2008) Spectral vegetation indices for benchmarking water productivity of irrigated cotton and sugarbeet crops. Agric Water Manag 95:48–58. https://doi.org/10.1016/j.agwat.2007.09.001

Griffel LM, Delparte D, Edwards J (2018) Using Support Vector Machines classification to differentiate spectral signatures of potato plants infected with Potato Virus Y. Comput Electron Agric 153:318–324. https://doi.org/10.1016/j.compag.2018.08.027

Gupta DS, Ibaraki Y, Pattanayak AK (2013) Development of a digital image analysis method for real-time estimation of chlorophyll content in micropropagated potato plants. Plant Biotechnol Rep 7:91–97. https://doi.org/10.1007/s11816-012-0240-5

Haboudane D, Miller JR, Tremblay N et al (2002) Integrated narrow-band vegetation indices for prediction of crop chlorophyll content for application to precision agriculture. Remote Sens Environ 81:416–426. https://doi.org/10.1016/S0034-4257(02)00018-4

Haboudane D, Miller JR, Pattey E et al (2004) Hyperspectral vegetation indices and novel algorithms for predicting green LAI of crop canopies: Modeling and validation in the context of precision agriculture. Remote Sens Environ 90:337–352. https://doi.org/10.1016/j.rse.2003.12.013

Han D, Yang H, Qiu C, Yang G, Chen E, Du Y, Yang W, Zhou C (2019) Estimating wheat biomass from GF-3 data and a polarized water cloud model. Remote Sens Lett 10:234–243. https://doi.org/10.1080/2150704X.2018.1542184

Haverkort AJ (2018) Potato handbook: Crop of the future. Aardappelwereld BV, The Hague

He L, Wang R, Mostovoy G, Liu J, Chen JM, Shang J, Liu J, McNairn H, Powers J (2021) Crop biomass mapping based on ecosystem modeling at regional scale using high resolution sentinel-2 data. Remote Sens 13:806. https://doi.org/10.3390/rs13040806

Herrmann I, Karnieli A, Bonfil DJ, Cohen Y, Alchanatis V (2010) SWIR-based spectral indices for assessing nitrogen content in potato fields. Int J Remote Sens 31:5127–5143. https://doi.org/10.1080/01431160903283892

Herrmann I, Pimstein A, Karnieli A, Cohen Y, Alchanatis V, Bonfil DJ (2011) LAI assessment of wheat and potato crops by VENμS and Sentinel-2 bands. Remote Sens Environ 115:2141–2151. https://doi.org/10.1016/j.rse.2011.04.018

Hirooka Y, Homma K, Maki M, Sekiguchi K (2015) Applicability of synthetic aperture radar (SAR) to evaluate leaf area index (LAI) and its growth rate of rice in farmers' fields in Lao PDR. F Crop Res 176:119–122. https://doi.org/10.1016/j.fcr.2015.02.022

Hoogenboom G, Porter CH, Boote KJ, Shelia V, Wilkens PW, Singh U, White JW, Asseng S, Lizaso JI, Moreno PL, Pavan W, Ogoshi R, Hunt LA, Tsuji GY, Jones JW (2019) Advances in crop modelling for a sustainable agriculture. In: Boote KJ (ed) Advances in crop modelling for a sustainable agriculture, 1st edn. Burleigh Dodds Science Publishing, Cambridge UK, pp 1–45

Hosseini M, McNairn H, Mitchell S et al (2019) Synthetic aperture radar and optical satellite data for estimating the biomass of corn. Int J Appl Earth Obs Geoinf 83:101933. https://doi.org/10.1016/j.jag.2019.101933

Hou B, Hu Y, Zhang P, Hou L (2022) Potato late blight severity and epidemic period prediction based on vis/nir spectroscopy. Agric 12:897. https://doi.org/10.3390/agriculture12070897

Huete AR (1988) A soil-adjusted vegetation index (SAVI). Remote Sens Environ 25:295–309

Irmak A, Ratcliffe I, Ranade P et al (2011) Estimation of land surface evapotranspiration with a satellite remote sensing procedure. Gt Plains Res 21:73–88

Jain N, Ray SS, Singh JP, Panigrahy S (2007) Use of hyperspectral data to assess the effects of different nitrogen applications on a potato crop. Precis Agric 8:225–239. https://doi.org/10.1007/s11119-007-9042-0

Jayanthi H, Neale CMU, Wright JL (2007) Development and validation of canopy reflectance-based crop coefficient for potato. Agric Water Manag 88:235–246. https://doi.org/10.1016/j.agwat.2006.10.020

Jimenez-Berni JA, Deery DM, Rozas-Larraondo P et al (2018) High throughput determination of plant height, ground cover, and above-ground biomass in wheat with LiDAR. Front Plant Sci 9:1–18. https://doi.org/10.3389/fpls.2018.00237

Jin X, Yang G, Xu X et al (2015) Combined multi-temporal optical and radar parameters for estimating LAI and biomass in winter wheat using HJ and RADARSAR-2 data. Remote Sens 7:13251–13272. https://doi.org/10.3390/rs71013251

Jin X, Kumar L, Li Z et al (2016) Estimation of winter wheat biomass and yield by combining the aquacrop model and field hyperspectral data. Remote Sens 8:1–15. https://doi.org/10.3390/rs8120972

Jin X, Kumar L, Li Z et al (2018) A review of data assimilation of remote sensing and crop models. Eur J Agron 92:141–152. https://doi.org/10.1016/j.eja.2017.11.002

Jin X, Zarco-Tejada PJ, Schmidhalter U et al (2021) High-throughput estimation of crop traits: A review of ground and aerial phenotyping platforms. IEEE Geosci Remote Sens Mag 9:200–231. https://doi.org/10.1109/MGRS.2020.2998816

Johnson DM (2016) A comprehensive assessment of the correlations between field crop yields and commonly used MODIS products. Int J Appl Earth Obs Geoinf 52:65–81. https://doi.org/10.1016/j.jag.2016.05.010

Kasampalis DA, Alexandridis TK, Deva C et al (2018) Contribution of remote sensing on crop models: A review. J Imaging 4:1–19. https://doi.org/10.3390/jimaging4040052

Khabbazan S, Vermunt P, Steele-Dunne S et al (2019) Crop monitoring using Sentinel-1 data: A case study from The Netherlands. Remote Sens 11:1887. https://doi.org/10.3390/rs11161887

Khanal S, Kc K, Fulton JP et al (2020) Remote Sensing in agriculture — accomplishments, limitations, and opportunities. Remote Sens 12:1–29

Kitchenham BA, Charters S (2007) Guidelines for performing systematic literature reviews in software engineering version 2.3. Engineering 45(4ve):1051

Kooistra L, Clevers JGPW (2016) Estimating potato leaf chlorophyll content using ratio vegetation indices. Remote Sens Lett 7:611–620. https://doi.org/10.1080/2150704X.2016.1171925

Kumar P, Dubey S, Kimothi MM, Mamatha S, Ray SS (2019) Analysis of remote sensing-based assessment of potato statistics and its comparison with government estimates. Int Arch Photogramm Remote Sens Spatial Inf Sci 42:299–305

Kumar U, Sahoo B, Chatterjee C, Raghuwanshi NS (2020) Evaluation of simplified surface energy balance index (S-SEBI) method for estimating actual evapotranspiration in Kangsabati Reservoir Command using Landsat 8 imagery. J Indian Soc Remote Sens 48:1421–1432. https://doi.org/10.1007/s12524-020-01166-9

Launay M, Guerif M (2005) Assimilating remote sensing data into a crop model to improve predictive performance for spatial applications. Agric Ecosyst Environ 111:321–339. https://doi.org/10.1016/j.agee.2005.06.005

Li W, Niu Z, Huang N et al (2015) Airborne LiDAR technique for estimating biomass components of maize: A case study in Zhangye City, Northwest China. Ecol Indic 57:486–496. https://doi.org/10.1016/j.ecolind.2015.04.016

Li B, Xu X, Zhang L et al (2020a) Above-ground biomass estimation and yield prediction in potato by using UAV-based RGB and hyperspectral imaging. ISPRS J Photogramm Remote Sens 162:161–172. https://doi.org/10.1016/j.isprsjprs.2020.02.013

Li C, Chen P, Ma C et al (2020b) Estimation of potato chlorophyll content using composite hyperspectral index parameters collected by an unmanned aerial vehicle. Int J Remote Sens 41:8176–8197. https://doi.org/10.1080/01431161.2020.1757779

Li C, Ma C, Pei H et al (2020c) Estimation of potatobiomass and yield based on machine learning from hyperspectral remote sensing data. J Agric Sci Technol B 10:195–213. https://doi.org/10.17265/2161-6264/2020.04.001

Li C, Ma C, Chen P et al (2021a) Machine learning-based estimation of potato chlorophyll content at different growth stages using uav hyperspectral data. Zemdirbyste-Agriculture 108:181–190. https://doi.org/10.13080/z-a.2021.108.024

Li D, Miao Y, Gupta SK et al (2021b) Improving potato yield prediction by combining cultivar information and uav remote sensing data using machine learning. Remote Sens 13:3322–3340. https://doi.org/10.3390/rs13163322

Liberati A, Altman DG, Tetzlaff J et al (2009) The PRISMA statement for reporting systematic reviews and meta-analyses of studies that evaluate health care interventions: explanation and elaboration. Ann Intern Med 151:65–94. https://doi.org/10.1016/j.jclinepi.2009.06.006

Liu N, Townsend PA, Naber MR et al (2021) Hyperspectral imagery to monitor crop nutrient status within and across growing seasons. Remote Sens Environ 255:112303–112326. https://doi.org/10.1016/j.rse.2021.112303

Liu Y, Feng H, Yue J et al (2022a) Estimation of potato above-ground biomass using UAV-based hyperspectral images and machine-learning regression. Remote Sens 14:1–19. https://doi.org/10.3390/rs14215449

Liu Y, Feng H, Yue J et al (2022b) Remote-sensing estimation of potato above-ground biomass based on spectral and spatial features extracted from high-definition digital camera images. Comput Electron Agric 198:107089–107102. https://doi.org/10.1016/j.compag.2022.107089

Liu Y, Feng H, Yue J et al (2022c) Estimation of potato above-ground biomass based on unmanned aerial vehicle red-green-blue images with different texture features and crop height. Front Plant Sci 13:1–18. https://doi.org/10.3389/fpls.2022.938216

Liu Y, Feng H, Yue J et al (2022d) Estimation of potato above-ground biomass based on vegetation indices and green-edge parameters obtained from UAVs. Remote Sens 14:1–17. https://doi.org/10.3390/rs14215323

Liu Y, Feng H, Yue J et al (2022e) Estimation of aboveground biomass of potatoes based on characteristic variables extracted from UAV hyperspectral imagery. Remote Sens 14:1–27. https://doi.org/10.3390/rs14205121

Lobell DB (2013) The use of satellite data for crop yield gap analysis. F Crop Res 143:56–64. https://doi.org/10.1016/j.fcr.2012.08.008

Lobell DB, Ortiz-Monasterio JI, Falcon WP (2007) Yield uncertainty at the field scale evaluated with multi-year satellite data. Agric Syst 92:76–90. https://doi.org/10.1016/j.agsy.2006.02.010

Lu N, Zhou J, Han Z et al (2019) Improved estimation of aboveground biomass in wheat from RGB imagery and point cloud data acquired with a low-cost unmanned aerial vehicle system. Plant Methods 15:1–16. https://doi.org/10.1186/s13007-019-0402-3

Luo S, He Y, Li Q et al (2020) Nondestructive estimation of potato yield using relative variables derived from multi-period LAI and hyperspectral data based on weighted growth stage. Plant Methods 16:1–14. https://doi.org/10.1186/s13007-020-00693-3

Luo S, Jiang X, He Y et al (2022) Multi-dimensional variables and feature parameter selection for above-ground biomass estimation of potato based on UAV multispectral imagery. Front Plant Sci 13:1–13. https://doi.org/10.3389/fpls.2022.948249

Mandal D, Kumar V, McNairn H et al (2019) Joint estimation of Plant Area Index (PAI) and wet biomass in wheat and soybean from C-band polarimetric SAR data. Int J Appl Earth Obs Geoinf 79:24–34. https://doi.org/10.1016/j.jag.2019.02.007

Mao P, Qin L, Hao M et al (2021) An improved approach to estimate above-ground volume and biomass of desert shrub communities based on UAV RGB images. Ecol Indic 125:107494. https://doi.org/10.1016/j.ecolind.2021.107494

Marshall M, Thenkabail P (2015) Advantage of hyperspectral EO-1 Hyperion over multispectral IKONOS, GeoEye-1, WorldView-2, Landsat ETM+, and MODIS vegetation indices in crop biomass estimation. ISPRS J Photogramm Remote Sens 108:205–218. https://doi.org/10.1016/j.isprsjprs.2015.08.001

Mercier A, Betbeder J, Baudry J et al (2020) Evaluation of Sentinel-1 & 2 time series for predicting wheat and rapeseed phenological stages. ISPRS J Photogramm Remote Sens 163:231–256. https://doi.org/10.1016/j.isprsjprs.2020.03.009

Mhango JK, Harris WE, Monaghan JM (2021) Relationships between the spatio-temporal variation in reflectance data from the sentinel-2 satellite and potato (Solanum tuberosum l.) yield and stem density. Remote Sens 13:1–22. https://doi.org/10.3390/rs13214371

Mhango JK, Grove IG, Hartley W et al (2022) Applying colour-based feature extraction and transfer learning to develop a high throughput inference system for potato (Solanum tuberosum L.) stems with images from unmanned aerial vehicles after canopy consolidation. Precis Agric 23:643–669. https://doi.org/10.1007/s11119-021-09853-4

Moran MS, Hymer DC, Qi J, Kerr Y (2002) Comparison of ERS-2 SAR and Landsat TM imagery for monitoring agricultural crop and soil conditions. Remote Sens Environ 79:243–252. https://doi.org/10.1016/S0034-4257(01)00276-0

Morier T, Cambouris AN, Chokmani K (2015) In-season nitrogen status assessment and yield estimation using hyperspectral vegetation. Agron J 107:1295–1309

Mourad R, Jaafar H, Anderson M, Gao F (2020) Assessment of leaf area index models using harmonized Landsat and Sentinel-2 surface reflectance data over a semi-arid irrigated landscape. Remote Sens 12:3121–3156. https://doi.org/10.3390/RS12193121

Mukiibi A, Franke AC, Steyn JM (2023) Determination of crop coefficients and evapotranspiration of potato in a semi-arid climate using canopy state variables and satellite-based NDVI. Remote Sens 15:4579. https://doi.org/10.3390/rs15184579

Mulla DJ (2013) Twenty five years of remote sensing in precision agriculture: Key advances and remaining knowledge gaps. Biosyst Eng 114:358–371. https://doi.org/10.1016/j.biosystemseng.2012.08.009

Muruganantham P, Wibowo S, Grandhi S et al (2022) A Systematic literature review on crop yield prediction with deep learning and remote sensing. Remote Sens 14:1990–2011. https://doi.org/10.3390/rs14091990

Ndikumana E, Minh DHT, Nguyen HTD et al (2018) Estimation of rice height and biomass using multitemporal SAR Sentinel-1 for Camargue, Southern France. Remote Sens 10:1–18. https://doi.org/10.3390/rs10091394

Newton IH, Tariqul Islam AFM, Saiful Islam AKM et al (2018) Yield prediction model for potato using Landsat time series images driven vegetation indices. Remote Sens Earth Syst Sci 1:29–38. https://doi.org/10.1007/s41976-018-0006-0

Nguy-Robertson AL, Peng Y, Gitelson AA et al (2014) Estimating green LAI in four crops: Potential of determining optimal spectral bands for a universal algorithm. Agric for Meteorol 192–193:140–148. https://doi.org/10.1016/j.agrformet.2014.03.004

Nigon TJ, Mulla DJ, Rosen CJ et al (2014) Evaluation of the nitrogen sufficiency index for use with high resolution, broadband aerial imagery in a commercial potato field. Precis Agric 15:202–226. https://doi.org/10.1007/s11119-013-9333-6

Nigon TJ, Mulla DJ, Rosen CJ et al (2015) Hyperspectral aerial imagery for detecting nitrogen stress in two potato cultivars. Comput Electron Agric 112:36–46. https://doi.org/10.1016/j.compag.2014.12.018

Niu Y, Zhang L, Zhang H et al (2019) Estimating above-ground biomass of maize using features derived from UAV-based RGB imagery. Remote Sens 11:1261

Pei H, Feng H, Li C, Yang G, Wu Z, Liu M (2019) Estimation of aboveground biomass of potato based on ground hyperspectral. In 2019 8th International Conference on Agro-Geoinformatics (Agro-Geoinformatics). IEEE, pp 1–4

Peng J, Manevski K, Kørup K et al (2021a) Random forest regression results in accurate assessment of potato nitrogen status based on multispectral data from different platforms and the critical concentration approach. F Crop Res 268:108158. https://doi.org/10.1016/j.fcr.2021.108158

Peng J, Manevski K, Kørup K et al (2021b) Environmental constraints to net primary productivity at northern latitudes: A study across scales of radiation interception and biomass production of potato. Int J Appl Earth Obs Geoinf 94:1–12. https://doi.org/10.1016/j.jag.2020.102232

Pinter PJ, Hatfield JL, Schepers JS, Barnes EM, Moran MS, Daughtry CST, Upchurch DR (2003) Remote sensing for crop management. Photogramm Eng Remote Sensing 69:647–664. https://doi.org/10.14358/pers.69.6.647

Pôças I, Calera A, Campos I, Cunha M (2020) Remote sensing for estimating and mapping single and basal crop coefficientes: A review on spectral vegetation indices approaches. Agric Water Manag 233:106081. https://doi.org/10.1016/j.agwat.2020.106081

Polder G, Blok PM, de Villiers HAC, van der Wolf JM, Kamp J (2019) Potato virus Y detection in seed potatoes using deep learning on hyperspectral images. Front Plant Sci 10:1–13. https://doi.org/10.3389/fpls.2019.00209

Poley LG, McDermid GJ (2020) A systematic review of the factors influencing the estimation of vegetation aboveground biomass using unmanned aerial systems. Remote Sens 12:1052. https://doi.org/10.3390/rs12071052

Poorter H, Niklas KJ, Reich PB, Oleksyn J, Poot P, Mommer L (2012) Biomass allocation to leaves, stems and roots: Meta-analyses of interspecific variation and environmental control. New Phytol 193:30–50. https://doi.org/10.1111/j.1469-8137.2011.03952.x

Prasad AK, Chai L, Singh RP, Kafatos M (2006) Crop yield estimation model for Iowa using remote sensing and surface parameters. Int J Appl Earth Obs Geoinf 8:26–33. https://doi.org/10.1016/j.jag.2005.06.002

Rahman A, Kaisar K, Krakauer NY, Roytman L, Kogan F (2012) Using AVHRR-based vegetation health indices for estimation Of potato yield in Bangladesh. J Civ Environ Eng 02:10–13. https://doi.org/10.4172/2165-784x.1000111

Ray SS, Das G, Singh JP, Panigrahy S (2006) Evaluation of hyperspectral indices for LAI estimation and discrimination of potato crop under different irrigation treatments. Int J Remote Sens 27:5373–5387. https://doi.org/10.1080/01431160600763006

Raymundo R, Asseng S, Cammarano D, Quiroz R (2014) Potato, sweet potato, and yam models for climate change: A review. F Crop Res 166:173–185. https://doi.org/10.1016/j.fcr.2014.06.017

Roosjen PPJ, Brede B, Suomalainen JM, Bartholomeus HM, Kooistra L, Clevers JGPW (2018) Improved estimation of leaf area index and leaf chlorophyll content of a potato crop using multi-angle

spectral data – potential of unmanned aerial vehicle imagery. Int J Appl Earth Obs Geoinf 66:14–26. https://doi.org/10.1016/j.jag.2017.10.012

Roth L, Streit B (2018) Predicting cover crop biomass by lightweight UAS-based RGB and NIR photography: an applied photogrammetric approach. Precis Agric 19:93–114. https://doi.org/10.1007/s11119-017-9501-1

Salvador P, Gómez D, Sanz J, Casanova JL (2020) Estimation of potato yield using satellite data at a municipal level: A machine learning approach. ISPRS Int J Geo-Information 9:343–356. https://doi.org/10.3390/ijgi9060343

Satognon F, Lelei JJ, Owido SFO (2021) Use of GreenSeeker and CM-100 as manual tools for nitrogen management and yield prediction in irrigated potato (Solanum tuberosum L.) production. Arch Agric Environ Sci 6:121–128. https://doi.org/10.26832/24566632.2021.060202

Sharma LK, Bali SK, Dwyer JD, Plant AB, Bhowmik A (2017) A case study of improving yield prediction and sulfur deficiency detection using optical sensors and relationship of historical potato yield with weather data in Maine. Sensors (switzerland) 17:1–23. https://doi.org/10.3390/s17051095

Shu M, Li Q, Ghafoor A, Zhu J, Li B, Ma Y (2023) Using the plant height and canopy coverage to estimation maize aboveground biomass with UAV digital images. Eur J Agron 151:126957. https://doi.org/10.1016/j.eja.2023.126957

Singha C, Swain KC (2022) Evaluating the NDVI based rice and potato yield prediction map using GIS geostatistical environment. In 2022 Second International Conference on Advances in Electrical, Computing, Communication and Sustainable Technologies (ICAECT). IEEE, pp 1–7

Singha C, Swain KC, Jayasuriya H (2022) Growth and yield monitoring of potato crop using Sentinel-1 data through cloud computing. Arab J Geosci 15:1–16. https://doi.org/10.1007/s12517-022-10844-6

Steele-Dunne SC, McNairn H, Monsivais-Huertero A, Judge J, Liu PW, Papathanassiou K (2017) Radar remote sensing of agricultural canopies: A review. IEEE J Sel Top Appl Earth Obs Remote Sens 10:2249–2273. https://doi.org/10.1109/JSTARS.2016.2639043

Stone RC, Meinke H (2005) Operational seasonal forecasting of crop performance. Philos Trans R Soc B Biol Sci 360:2109–2124. https://doi.org/10.1098/rstb.2005.1753

Sun C, Feng L, Zhang Z, Ma Y, Crosby T, Naber M, Wang Y (2020) Prediction of end-of-season tuber yield and tuber set in potatoes using in-season uav-based hyperspectral imagery and machine learning. Sensors (switzerland) 20:1–13. https://doi.org/10.3390/s20185293

Sun C, Zhou J, Ma Y, Xu Y, Pan B, Zhang Z (2022) A review of remote sensing for potato traits characterization in precision agriculture. Front Plant Sci 13:1–20. https://doi.org/10.3389/fpls.2022.871859

Tanabe D, Ichiura S, Nakatsubo A, Kobayashi T, Katahira M (2019) Yield prediction of potato by unmanned aerial vehicle. TAE 2019 - Proceeding 7th Int Conf Trends Agric Eng 2:540–546

Tasumi M, Allen RG (2007) Satellite-based ET mapping to assess variation in ET with timing of crop development. Agric Water Manag 88:54–62. https://doi.org/10.1016/j.agwat.2006.08.010

Tasumi M, Allen RG, Trezza R, Wright JL (2005) Satellite-Based Energy Balance to Assess Within-Population Variance of Crop Coefficient Curves. J Irrig Drain Eng 131:94–109. https://doi.org/10.1061/(asce)0733-9437(2005)131:1(94)

ten Harkel J, Bartholomeus H, Kooistra L (2020) Biomass and crop height estimation of different crops using UAV-based Lidar. Remote Sens 12:1–18

Tenreiro TR, García-Vila M, Gómez JA, Jimenez-Berni JA, Fereres E (2021) Using NDVI for the assessment of canopy cover in agricultural crops within modelling research. Comput Electron Agric 182:1–12. https://doi.org/10.1016/j.compag.2021.106038

Ter Steege MW, Den Ouden FM, Lambers H, Stam P, Peeter JM (2005) Genetic and physiological architecture of early vigor in Aegilops tauschii, the D-genome donor of hexaploid wheat. A quantitative trait loci analysis. Plant Physiol 139:1078–1094. https://doi.org/10.1104/pp.105.063263

Tiedeman K, Chamberlin J, Kosmowski F, Ayalew H, Sida T, Hijmans RJ (2022) Field data collection methods strongly affect satellite-based crop yield estimation. Remote Sens 14:1–17. https://doi.org/10.3390/rs14091995

Turner D, Lucieer A, Watson C (2012) An automated technique for generating georectified mosaics from ultra-high resolution Unmanned Aerial Vehicle (UAV) imagery, based on Structure from Motion (SFM) point clouds. Remote Sens 4:1392–1410. https://doi.org/10.3390/rs4051392

Uddling J, Gelang-Alfredsson J, Piikki K, Pleijel H (2007) Evaluating the relationship between leaf chlorophyll concentration and SPAD-502 chlorophyll meter readings. Photosynth Res 91:37–46. https://doi.org/10.1007/s11120-006-9077-5

Van De Vijver R, Mertens K, Heungens K, Somers B, Nuyttens D, Borra-Serrano I, Lootens P, Roldan-Ruiz I, Vangeyte J, Saeys W (2020) In-field detection of Alternaria solani in potato crops using hyperspectral imaging. Comput Electron Agric 168:105106. https://doi.org/10.1016/j.compag.2019.105106

Van der Velde M, Nisini L (2019) Performance of the MARS-crop yield forecasting system for the European Union: Assessing accuracy, in-season, and year-to-year improvements from 1993 to 2015. Agric Syst 168:203–212. https://doi.org/10.1016/j.agsy.2018.06.009

van Eck NJ, Waltman L (2010) Software survey: VOSviewer, a computer program for bibliometric mapping. Scientometrics 84:523–538. https://doi.org/10.1007/s11192-009-0146-3

van Evert FK, Booij R, Jukema JN, ten Berge HFM, Uenk D, Meurs EJJB, van Geel WCA, Wijnholds KH, Slabbekoorn JJH (2012) Using crop reflectance to determine sidedress N rate in potato saves N and maintains yield. Eur J Agron 43:58–67. https://doi.org/10.1016/j.eja.2012.05.005

Vannoppen A, Gobin A (2022) Estimating Yield from NDVI, Weather Data, and Soil Water Depletion for Sugar Beet and Potato in Northern Belgium. Water (switzerland) 14:1–15. https://doi.org/10.3390/w14081188

Verrelst J, Rivera JP, Veroustraete F, Munoz-Mari J, Clevers JGPW, Camps-Valls G, Moreno J (2015) Experimental Sentinel-2 LAI estimation using parametric, non-parametric and physical retrieval methods - A comparison. ISPRS J Photogramm Remote Sens 108:260–272. https://doi.org/10.1016/j.isprsjprs.2015.04.013

Wan L, Zhang J, Dong X, Du X, Zhu J, Sun D, Liu Y, He Y, Cen H (2021) Unmanned aerial vehicle-based field phenotyping of crop biomass using growth traits retrieved from PROSAIL model. Comput Electron Agric 187:106304. https://doi.org/10.1016/j.compag.2021.106304

Weiss M, Jacob F, Duveiller G (2020) Remote sensing for agricultural applications: A meta-review. Remote Sens Environ 236:111402. https://doi.org/10.1016/j.rse.2019.111402

Wu J, Wang D, Bauer ME (2007) Assessing broadband vegetation indices and QuickBird data in estimating leaf area index of corn and potato canopies. F Crop Res 102:33–42. https://doi.org/10.1016/j.fcr.2007.01.003

Xue J, Su B (2017) Significant remote sensing vegetation indices: A review of developments and applications. J Sensors 1:1–17. https://doi.org/10.1155/2017/1353691

Yadav SP, Ibaraki Y, Gupta SD (2010) Estimation of the chlorophyll content of micropropagated potato plants using RGB based image analysis. Plant Cell Tissue Organ Cult 100:183–188. https://doi.org/10.1007/s11240-009-9635-6

Yang H, Li F, Wang W, Yu K (2021) Estimating above-ground biomass of potato using random forest and optimized hyperspectral indices. Remote Sens 13:1–19. https://doi.org/10.3390/rs13122339

Yang H, Hu Y, Zheng Z, Qiao Y, Zhang K, Guo T, Chen J (2022) Estimation of potato chlorophyll content from UAV multispectral images with stacking ensemble algorithm. Agronomy 12:1–16. https://doi.org/10.3390/agronomy12102318

Yin H, Huang W, Li F, Yang H, Li Y, Hu Y, Yu K (2022) Multi-temporal UAV imaging-based mapping of chlorophyll content in potato crop. PFG - J Photogramm Remote Sens Geoinf Sci 10:1–19. https://doi.org/10.1007/s41064-022-00218-8

Yu N, Li L, Schmitz N, Tian LF, Greenberg JA, Diers BW (2016) Development of methods to improve soybean yield estimation and predict plant maturity with an unmanned aerial vehicle based platform. Remote Sens Environ 187:91–101. https://doi.org/10.1016/j.rse.2016.10.005

Yue J, Feng H, Jin X, Yuan H, Li Z, Zhou C, Yang G, Tian Q (2018) A comparison of crop parameters estimation using images from UAV-mounted snapshot hyperspectral sensor and high-definition digital camera. Remote Sens 10:1138. https://doi.org/10.3390/rs10071138

Yue J, Yang G, Tian Q, Feng H, Xu K, Zhou C (2019) Estimate of winter-wheat above-ground biomass based on UAV ultrahigh-ground-resolution image textures and vegetation indices. ISPRS J Photogramm Remote Sens 150:226–244. https://doi.org/10.1016/j.isprsjprs.2019.02.022

Zaeen AA, Sharma L, Jasim A, Bali S, Buzza A, Alyokhin A (2020) In-season potato yield prediction with active optical sensors. Agrosystems, Geosci Environ 3:1–15. https://doi.org/10.1002/agg2.20024

Zhai W, Li C, Cheng Q, Mao B, Li Z, Li Y, Ding F, Qin S, Fei S, Chen Z (2023) Enhancing wheat above-ground biomass estimation using UAV RGB images and machine learning: Multi-feature combinations, flight height, and algorithm implications. Remote Sens 15:3653. https://doi.org/10.3390/rs15143653

Zhang C, Kovacs JM (2012) The application of small unmanned aerial systems for precision agriculture: A review. Precis Agric 13:693–712. https://doi.org/10.1007/s11119-012-9274-5

Zheng H, Cheng T, Zhou M, Li D, Yao X, Tian Y, Cao W, Zhu Y (2019) Improved estimation of rice aboveground biomass combining textural and spectral analysis of UAV imagery. Precis Agric 20:611–629. https://doi.org/10.1007/s11119-018-9600-7

Zhou X, Zheng HB, Xu XQ, He JY, Ge XK, Yao X, Cheng T, Zhu Y, Cao WX, Tian YC (2017a) Predicting grain yield in rice using multi-temporal vegetation indices from UAV-based multispectral and digital imagery. ISPRS J Photogramm Remote Sens 130:246–255. https://doi.org/10.1016/j.isprsjprs.2017.05.003

Zhou Z, Plauborg F, Thomsen AG, Andersen MN (2017b) A RVI/LAI-reference curve to detect N stress and guide N fertigation using combined information from spectral reflectance and leaf area measurements in potato. Eur J Agron 87:1–7. https://doi.org/10.1016/j.eja.2017.04.002

Zhou Z, Jabloun M, Plauborg F, Andersen MN (2018) Using ground-based spectral reflectance sensors and photography to estimate shoot N concentration and dry matter of potato. Comput Electron Agric 144:154–163. https://doi.org/10.1016/j.compag.2017.12.005

Zhou J, Wang B, Fan J, Ma Y, Wang Y, Zhang Z (2022) A systematic study of estimating potato N concentrations using UAV-based hyper- and multi-spectral imagery. Agronomy 12:1–16. https://doi.org/10.3390/agronomy12102533

Zhu W, Sun Z, Peng J, Huang Y, Li J, Zhang J, Yang B, Liao X (2019) Estimating maize above-ground biomass using 3D point clouds of multi-source unmanned aerial vehicle data at multi-spatial scales. Remote Sens 11:2678. https://doi.org/10.3390/rs11222678